CrossMark

Differential Impact of Anniversary-Severe Cyclones on the Water Quality of a Tropical Coastal Lagoon

Abhishek Kumar[1,2] · Deepak R. Mishra[1] · Sk. Md. Equeenuddin[2] ·
Hyun Jung Cho[3] · Gurdeep Rastogi[4]

Abstract Mapping spatio-temporal dynamics of suspended load in a lagoon before-during-after a cyclone is crucial for monitoring sudden nutrient enrichment and associated processes such as algal blooms and siltation. However, not all cyclones produce similar impact on a coastal lagoon, some trigger algal blooms after passage while others just increase the overall turbidity. Asia's largest brackish water lagoon, Chilika Lagoon, India was hit by two anniversary-severe cyclones *Phailin* (12 October 2013) and *Hudhud* (12 October 2014) recently. Their impacts were analysed with respect to physical, biological and meteorological factors which favour or restrict a phytoplankton bloom after the passage of a storm. Moderate-resolution imaging spectroradiometer surface reflectance data were used to examine the spatio-temporal variability in total suspended sediment (TSS) and chlorophyll-*a* (Chl-*a*) concentration pre- and post-cyclone. Comparative results revealed that *Phailin* was associated with higher rainfall, wind speed and surface runoff compared with *Hudhud*. These factors contributed to higher TSS concentration in all sectors of the lagoon post-*Phailin* compared with post-*Hudhud*.

Extreme TSS, limited light, high rainfall and runoff and increased flushing rate post-*Phailin* restricted the likelihood of a phytoplankton bloom in the lagoon, a commonly reported phenomenon after the passage of a cyclone. In contrast, sufficient light availability due to lower TSS, low runoff and flushing and stable wind supported a phytoplankton bloom post-*Hudhud*. The observed differential impacts were linked to the individual cyclone's characteristics such as differences in landfall locations, wind speed, trajectory after the landfall, differences in rainfall rate and surface runoff and speed of passage.

Keywords Cyclone · Phailin · Hudhud · MODIS · Giovanni · Chilika · Suspended sediment · Chlorophyll-*a* · Algal bloom

✉ Deepak R. Mishra
  dmishra@uga.edu

[1] Department of Geography, University of Georgia, 210 Field Street, Room 204, Athens, GA 30602, USA

[2] Department of Earth and Atmospheric Sciences, National Institute of Technology, Rourkela, Odisha 769008, India

[3] Department of Integrated Environmental Science, Bethune-Cookman University, 640 Dr. Mary McLeod Bethune Blvd, Daytona Beach, FL 32114, USA

[4] Wetland Research and Training Centre, Chilika Development Authority, Barkul, Balugaon, Odisha 751014, India

Introduction

Estuaries, lagoons and surrounding watershed can experience extreme wind velocities, storm surges and rainfall during hurricanes or cyclones, resulting in strong water column mixing, variability in flow regime and modification in local geomorphology (Peierls et al. 2003). These episodic weather events also cause strong sediment re-suspension in the water column (Chen et al. 2009), which may temporarily alter the overall water quality of an aquatic system and associated biological, chemical and geomorphological processes (Miller et al. 2011). In addition, cyclones facilitate substantial nutrient loading from the surrounding areas that can trigger algal blooms, reduce water clarity and increase hypoxic zones in the lakes and estuaries (Peierls et al. 2003; Miller et al. 2006; Paerl et al. 2006). Besides, increasing the sediment load and stimulating algal blooms, such extreme events are often associated with heavy floodwaters entering the estuaries and altering the overall salinity gradient, if any (Paerl et al. 2001; Peierls et al.

🖄 Springer

2003; Srichandan et al. 2015b). For example, Sahoo et al. (2014) and Srichandan et al. (2015b) reported that the salinity in the Chilika Lagoon was reduced by 4-fold after cyclone *Phailin*. Monitoring the effects of such episodic events helps in understanding the movements and changes in suspended sediments, phytoplankton, deposition of non-living organism and the pollutants into lakes, estuaries and coastal water bodies (Dickey et al. 1998).

Do all cyclones produce similar impact on coastal lakes/ lagoons? If not, what factors play a role in determining the type of impact? An individual cyclone's characteristics is obviously one set of factors, what about watershed characteristics and lake optical property? Why some cyclones trigger algal blooms in a lagoon after their passage and some do not? These are some of the questions which shaped the framework of this research. Although numerous studies have provided explanations to the aforementioned questions, review of the literature showed contradictory findings regarding a lagoon's response aftermath a cyclone. For example, studies conducted in the past for assessing the impacts of storm events on lakes, estuaries and lagoons have revealed substantial changes in total suspended sediment (TSS) concentration (Chen et al. 2009; Havens et al. 2011; Kumar et al. 2016), turbidity (Wang et al. 2012) and phytoplankton biomass (Zhu et al. 2014; Paerl et al. 2001; Peierls et al. 2003; Paerl et al. 2006; Mallin et al. 2006; Mishra and Mishra 2010; Huang et al. 2011). Chen et al. (2009) observed that the mean TSS concentration in Apalachicola Bay, Florida, USA was almost three times higher post-hurricane *Frances* than that of pre-hurricane condition. Similar increase in TSS concentration (more than 2-fold) was reported by Kumar et al. (2016) in Chilika Lagoon, India after the passage of cyclone *Phailin*. Havens et al. (2011) also found 5-fold increase in suspended sediment concentration (SSC) in Lake Okeechobee, Florida, USA after the passage of hurricane *Frances* and *Jeanne*. Wang et al. (2012) studied the variability in turbidity over Lake Okeechobee after the passage of subsequent Hurricanes (*Charley*: 13 August 2004; *Frances*: 5 September 2004; *Ivan*: 20 September 2004 and *Jeanne*: 26 September 2004). They observed that the impact of Hurricane *Frances* on the lake's turbidity levels doubled post-hurricane due to persistent high wind speeds mixing and disturbing the lake sediments. However, they did not quantify the differential impacts of subsequent cyclones.

Every hurricane or cyclone is associated with different characteristics and delivers variable intensities of the impact based on its strength, landfall location, wind speed, amount of precipitation, speed of passage and trajectory after landfall (Mallin et al. 2002). Despite the differences in magnitude, a general consensus is found in the literature about the impact of hurricanes on coastal waterbodies resulting in immediate increase in suspended sediment load, reduced water clarity and reduced salinity. Similarly, numerous studies have reported a significant increase in phytoplankton biomass in coastal waterbodies after the passage of a hurricane. However, a general consensus was not found in the literature unlike findings on turbidity or water clarity.

Hurricane-induced phytoplankton blooms can occur rapidly after the passage due to a combination of forcings such as storm surge, ebb tide, heavy rainfall-induced flood, river flux, wind-driven water mixing and coastal runoff-induced nutrient pulsing (Paerl et al. 2001, 2006; Peierls et al. 2003; Mallin et al. 2006; Mishra and Mishra 2010; Huang et al. 2011; Sarangi et al. 2014; Angles et al. 2015). For example, Zhu et al. (2014) reported enhanced phytoplankton biomass (200,000 cells/mL) and toxic cyanobacteria blooms in Lake Taihu, China, post-cyclone *Muifa* and *Haikui* primarily due to the combined effect of nutrient pulsing, elevated water temperatures and increased water column stratification. Also, Sarangi et al. (2014) observed significant increase in Chl-*a* concentration post-*Phailin* (0.8–2.0 µg/L) compared with pre-*Phailin* Chl-*a* (0.1–0.6 µg/L) in Bay of Bengal (BOB). Huang et al. (2011) showed an increase of more than twice the mean Chl-*a* concentration (5.3–14.7 g/L) after Hurricane *Ivan* in Pensacola Bay, Florida. These studies reported a widely varying temporal lag of phytoplankton responses to tropical cyclones in estuaries and coastal lagoons from days to several weeks depending in light availability and intensity of flushing (Angles et al. 2015; Fogel et al. 1999; Lin et al. 2003; Babin et al. 2004; Wetz and Yoskowitz 2013). For instance, Huang et al. (2011) demonstrated a significant increase in phytoplankton concentration in Pensacola Bay only just after a day of passage of Hurricane *Ivan*. On the other hand, a wide temporal variability in long-term effects on coastal waters ranging from months to years have been reported after the passage of hurricanes (Paerl et al. 2010; Peierls et al. 2003).

Despite a significant number of studies showing immediate to gradual increase in phytoplankton abundance and biomass in coastal waterbodies after hurricanes, few studies reported somewhat contradictory results and findings. For instance, Mallin et al. (2002) reported a decrease in phytoplankton biomass in the lower Cape Fear estuary, North Carolina after hurricanes *Fran* (1996), *Bonnie* (1998) and *Floyd* (1999) primarily because of increased light attenuation. Similarly, Havens et al. (2011) observed 50 % reduction in plankton biomass in Lake Okeechobee post-hurricane period. They concluded that major cause of change in plankton dynamics was attenuation of light due to increased sediment re-suspension. Angles et al. (2015) assumed that rapid decrease in salinity post-hurricanes (Hurricane *Alex*, Hurricane *Karl*, Cyclone *Hermine* and tropical depressions) due to increased flushing might have restricted the buildup of phytoplankton biomass in estuarine systems (Guadalupe estuary, Mission-Arnasas estuary, Nueces estuary) near the Gulf of Mexico. They also concluded that other factors such as environmental conditions of the estuary pre- and post-hurricane, physical

nature of the estuarine system such as geometry and bathymetry can also influence the phytoplankton response. Most of the aforementioned studies incorporated a combination of field, modelled and satellite data acquired over several days after the passage of hurricanes to assess the impacts of the extreme events on water quality of lakes, estuaries and coastal areas (Paerl et al. 2001, 2006; Nayak et al. 2001; Chen et al. 2009; Miller et al. 2011; Wang et al. 2012; Wetz and Paerl 2008; Zhu et al. 2014; Sahoo et al. 2014; Sarangi et al. 2014; Mallin and Corbrett 2006; Angles et al. 2015; Havens et al. 2011; Huang et al. 2011; Mallin et al. 2002; Srichandan et al. 2015b; Kumar et al. 2016; Peierls et al. 2003). Satellite data can be very useful in such extreme environmental conditions for day-to-day monitoring when field sampling becomes impractical, particularly if model-derived products from satellite sensors (such as surface precipitation and surface runoff products) can be used to complement the satellite data.

This paper investigated and compared the impact of two anniversary very severe cyclonic storms (VSCSs) on a tropical coastal lagoon, Chilika, the largest brackish water lagoon in Asia. Two anniversary VSCSs, category-5 *Phailin* (12 October 2013) and category-4 *Hudhud* (12 October 2014), made landfalls at different proximities to the lagoon and followed different paths after the landfall (Fig. 1). The impact of the anniversary VSCSs on water quality (TSS, and phytoplankton biomass or chlorophyll: Chl-*a*) of the lagoon was assessed using a combination of satellite and meteorological data. National Aeronautics and Space Administration (NASA)'s Moderate Resolution Imaging Spectroradiometer (MODIS) surface reflectance products (MOD09GQ) and true colour images were analysed in combination with Geospatial Interactive Online Visualization ANd aNalysis Infrastructure (Giovanni)-derived precipitation, surface wind speed and surface runoff data to model spatio-temporal dynamics of TSS and Chl-*a* before-during-after the VSCSs.

Water quality parameters such as TSS (Miller and McKee 2004; Binding et al. 2005; Liu et al. 2006; Zhang et al. 2010; Tarrant et al. 2010; Zhao et al. 2011; Chen et al. 2011; Ondrusek et al. 2012; Cui et al. 2013; Wu et al. 2013), turbidity (Chen et al. 2007; Petus et al. 2010; Dogliotti et al. 2015) and Chl-*a* (Gitelson et al. 2003; Kahru et al. 2004; Zhang et al. 2011; Mishra and Mishra 2012; El-Alem et al. 2012; Srichandan et al. 2015b) have been estimated using MODIS two 250 m bands in numerous studies. Some of the studies have used MODIS products to show the impact of cyclonic events on water quality parameters of costal environments (Loherenz et al. 2008: Hurricane *Katrina*; Zhu et al. 2014: Cyclone *Muifa* and *Haikui*; Chen et al. 2009: Hurricane *Frances*; Shi and Wang 2008: Cyclone *Nargis*; Matarrese et al. 2005: Hurricane *Isabel*; Srichandan et al. 2015b: Cyclone *Phailin*). Chen et al. (2009) used MODIS Terra and Aqua 250 m data products (MOD02QKM and MYD02QKM) to show the variation in TSS concentration during-pre-post-

Hurricane *Frances* in Apalachicola Bay. They implemented a re-parameterised logarithmic-polynomial regression model (R^2, 0.8534; $n = 25$) using band ratio (band 2/band 1) to generate MODIS TSS maps. Wang et al. (2012) used MODIS band 2 (865 nm) to observe the variability in turbidity over Lake Okeechobee after the passage of subsequent Hurricanes (*Charley*: 13 August 2004; *Frances*: 5 September 2004; *Ivan*: 20 September 2004 and *Jeanne*: 26 September 2004). Matarrese et al. (2005) used a linear regression model (R, 0.8166) on MODIS data to show the variations in TSS concentration over Chesapeake Bay after Hurricane *Isabel*. Lahet and Stramski (2010) used MODIS band 1 (645 nm) and band 4 (555 nm) to demarcate the turbid plumes in San Diego coastal waters after several rainstorm events. Zhu et al. (2014) used Floating Algal Index (FAI) developed by Hu (2009) to map the algal bloom areas in Lake Taihu, China using MODIS images for 12 typhoons which passed over the lake in 7 years (January 2005–January 2012). However, none of these studies have evaluated the differential impacts of two anniversary cyclones making the landfall at different distances from a lake with different wind intensities.

Srichandan et al. (2015b) concluded that impacts of a cyclone depend not only on the geographic-geomorphologic-bathymetric setting of lagoons but also on individual hurricane characteristics. The landfall of the anniversary VSCSs at close proximity to the same lagoon in subsequent years provided the opportunity to formulate and test a hypothesis that the likelihood of a phytoplankton bloom or significant increase in phytoplankton biomass after a cyclone will be dependent on several factors such as category of the cyclone, point of landfall, wind speed, amount of rainfall and path after landfall. The two anniversary VSCSs were of different intensities and made landfall at different proximities to the lagoon which may have triggered differential impact on the water quality and surrounding geomorphology. Therefore, this study took the opportunity to evaluate all factors contributing to the variability in water quality for proper assessment of the impact of such extreme events. To the best of our knowledge, this is first of its kind study that analysed the differential impact of two anniversary VSCSs on the same lagoon using high temporal satellite and meteorological data to determine the likelihood of a bloom in a coastal water body after the passage of a hurricane/cyclone.

Study Area

Chilika Lagoon is located on the east coast of India at latitude ranging from 19° 28′ to 19° 54′ and longitude ranging from 85° 06′ to 85° 35′ along the Odisha coast and connected to the BOB through an outer channel (Fig. 1). The surface water area of the lagoon varies from 704 to 1020 km² during summer and monsoon season respectively (Gupta et al. 2008). Chilika
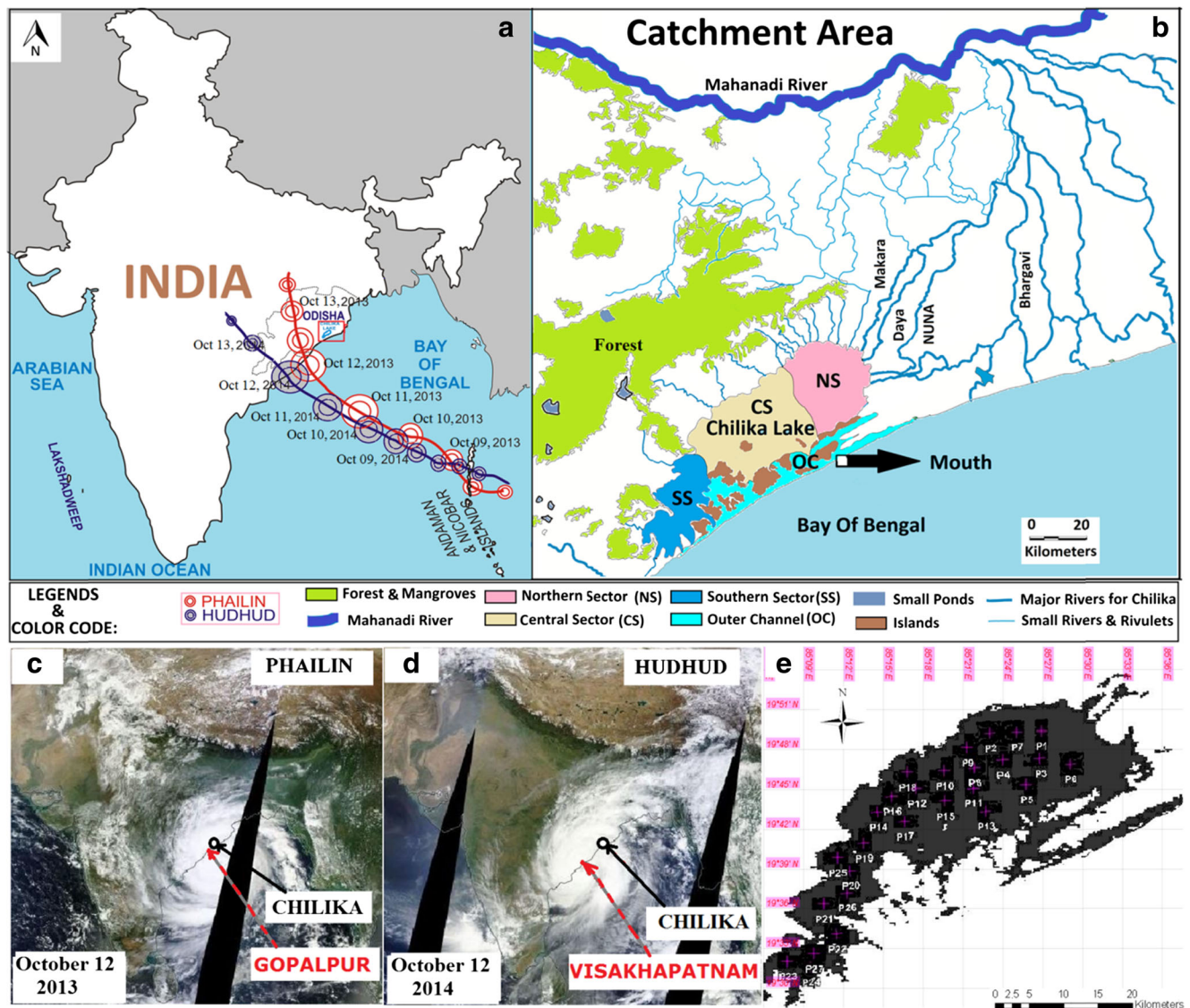
Fig. 1 Track of the two VSCSs (*Phailin*: *red line* and *Hudhud*: *blue line*) with respect to Chilika Lagoon (**a**). Map of study area showing different sectors (Northern sector (*NS*), Central sector (*CS*), Southern sector (*SS*) and Outer channel (*OC*)) of the lagoon and major distributaries of Mahanadi River into the lagoon (**b**); mouth in OC that connects the lagoon to the Bay of Bengal is also indicated using a *black arrow*. The landfall locations of two VSCSs are indicated by *red dashed arrow* with respect to Chilika Lagoon (*open circle*) (**c**, **d**). MODIS image (MOD09GQ) with sampling locations used for quantitative analysis of TSS and Chl-*a* in different sectors of the lagoon (**e**)

Lagoon is surrounded by three districts of Odisha namely, Puri, Khurda and Ganjam (Sahoo et al. 2014). These districts are the areas that received the most rainfall during and after VSCS *Phailin* (GoO 2013). The drainage area of lagoon is 3560 km^2; and it receives freshwater from 52 rivers and rivulets (Srichandan et al. 2015a). Some of the tributaries of Mahanadi River, the major source of fresh water to the lagoon, are shown in Fig. 1b. Western side of the lagoon is surrounded by hilly mountains and forests, whereas, the northern side is primarily dominated by rivers and rivulets (Fig. 1b). The lagoon is divided into four ecological sectors (Srichandan et al. 2015a), namely northern sector (NS), central sector (CS), southern sector (SS) and outer channel (OC) based on salinity

gradient and depth (Fig. 1b). The NS experiences lower salinity (<5) as it is directly connected to the tributaries of Mahanadi River, CS exhibits variable salinity (6–15) due to fresh water and seawater exchange, SS exhibits higher (>15) and stable salinity and OC experiences highest salinity (>30) because of its direct connectivity with BOB (Srichandan et al. 2015b). Chilika Lagoon also exhibits variable turbidity (proxy of TSS) regime in different sectors along with variability in depth such as highest turbidity in NS (annual mean TSS, 63–101 mg/L) with shallowest depth (0.6 m) and lowest turbidity range (Annual Mean TSS: 15–42 mg/L) in SS with highest depth (3 m) (Kumar et al. 2016; Gupta 2013). The average annual rainfall in lagoon area is 1238 mm. On the landfall day

of *Phailin,* lagoon received heavy precipitation of about 160 mm (Sahoo et al. 2014) and 80 mm on the landfall day of *Hudhud* (Baliarsingh et al. 2015).

VSCS Characteristics

Figure 1a shows the trajectories of VSCS *Phailin* and *Hudhud*. *Phailin* struck the Odisha coast on 12 October 2013 around 2230 hours Indian Standard Time (IST; 1700 hours UTC) with the maximum wind velocity reaching up to 220 km/h (IMD 2013). This VSCS was classified as category 5 on the Saffir-Simpson scale as per the norms of National Oceanic and Atmospheric Administration (NOAA). It was the second strongest tropical cyclone in the recorded history to make landfall in India only after the super cyclone of Odisha which struck the same area in 1999 with wind speed up to 260 km/h (IFRC 1999). Initially, a low pressure was formed in South China Sea on 06 October 2013 which further intensified into cyclonic storm on 09 October 2013 moving west-northwestwardly. It further intensified into a VSCS by moving northwestwardly on 10 October and finally made landfall on October 12 near Gopalpur district in Odisha (IMD 2013). The landfall location of VSCS *Phailin* was only 45 km southwest from Chilika Lagoon. The landfall of *Phailin* brought torrential rain and storm surges up to 3.5 m to the eastern Indian states of Odisha and Andhra Pradesh (UNEP 2013). The major districts of Odisha adjacent to the lagoon which encountered heavy rainfall during the 6 days (9–14 October) were Khurdha (273.3 mm), Nayagarh (261.8 mm), Ganjam (241.1 mm) and Puri (221.6 mm) according to report by Government of Odisha, India (GoO 2013). On the day of *Phailin* landfall (12 October 2013), the rainfall data recorded at the above locations were 67.76 % (185.2 mm), 76.96 % (201.5 mm), 75.91 % (183 mm) and 48.05 % (106.5 mm) of the cumulative 6 days rainfall at the corresponding locations (GoO 2013).

The second VSCS *Hudhud*, made landfall on 12 October 2014 near Visakhapatnam, Andhra Pradesh, exactly 1 year after VSCS *Phailin*. The landfall location was at a distance of 338 km southwest from Chilika Lagoon. This tropical cyclone was categorised as category 4 cyclone on the Saffir-Simpson scale. The maximum sustained wind speed during its landfall was about 185 km/h (IMD 2014). The states affected by heavy rainfall followed by VSCS *Hudhud* included North Andhra Pradesh, South Odisha, Chhattisgarh, East Uttar Pradesh, East Madhya Pradesh, Jharkhand and Bihar (IMD 2014). These VSCSs, *Phailin* and *Hudhud*, were very similar in their characteristics as both originated in the North Andaman Sea and moved almost in parallel path but there was a relatively small difference in strength, wind speed, landfall location and passage within the catchment after the landfall (Table 1; Mishra and Panigrahi 2014). Both VSCSs produced high negative economic impact, and a large number of fatalities reported only during VSCS *Hudhud* compared with VSCS *Phailin* as it struck the areas with high population densities and larger cities (Table 1) (IMD 2013 and 2014).

Methods

MODIS Data Processing

MODIS data products were obtained from NASA Goddard Space Flight Center's (GSFC) Level 1 and Atmosphere Archive and Distribution System (LAADS) FTP site (http://ladsweb.nascom.nasa.gov/data). In this study, MODIS Terra's 250-m surface reflectance (R_{rs}) products (MOD09GQ) were used along with MODIS true colour images. The true colour images were downloaded from NASA's GSFC Worldview website (https://earthdata.nasa.gov/labs/worldview/). High temporal resolution, precise geolocational accuracy and frequent revisit time, make MODIS an ideal satellite sensor to study high-frequency phenomenon such as cyclone impact. In addition, MOD09GQ contains atmospherically corrected surface reflectance values in band 1 (645 nm) and band 2 (859 nm) which eliminates the complexity of atmospheric correction procedure typically required in water quality studies. These bands have sufficient sensitivity to detect a wide range of colour in estuarine waters (Hu et al. 2004).

To process the MODIS products, Sea viewing Wide Field of view Sensor (SeaWiFS) Data Analysis System (SeaDAS) software available at NASA's ocean colour website (http://seadas.gsfc.nasa.gov/) was used. Visual quality check was performed to flag out images with substantive missing data patches and cloud cover. All MODIS images were corrected for spatial distortion by re-projecting them from sinusoidal coordinate system to geographical coordinate system (WGS 84). A geometrical mask was used for extracting the Chilika Lagoon data from all MODIS images. An additional mask used in the previous study by Kumar et al. (2016), which included a band ratio of remote sensing reflectance (R_{rs}) of band 2 and band 1 (R_{rs} (859 nm)/R_{rs} (645 nm) > 1.5), was used to mask out the islands present inside the lagoon which could not be eliminated using the first geometrical mask.

TSS and Chl-*a* Estimation

MOD09GQ data were used for extracting TSS and Chl-*a* concentrations to analyse their spatio-temporal variability in Chilika Lagoon pre- and post-cyclones. The MODIS based TSS and Chl-*a* models used in this study were developed recently by the authors using a comprehensive set of field data and coincident MODIS images (Kumar et al. 2016; Srichandan et al. 2015b). TSS and Chl-*a* concentration were

Table 1 Comparative description of anniversary VSCSs (*Phailin* and *Hudhud*)

Parameters	Phailin	Hudhud
Origin location with date	Gulf of Thailand and adjoining North Andaman Sea (6 October 2013; 9.5° N, 102.00° E)	Tenasserim coast and adjoining North Andaman Sea (6 October 2014; 10° N, 96° E)
Landfall location	Gopalpur, Odisha (19.27° N, 84.92° E)	Visakhapatnam, Andhra Pradesh (17.69° N, 83.22° E)
Distance (direction) from Chilika	45 km (southwest of Chilika)	338 km (southwest of Chilika)
Duration (stay over land)	~5 days	~3 days
Landfall date with time	12 October 2013 (22:30 IST)	12 October 2014 (between 12:00 and 13:00 IST)
Category	Category 5	Category 4
Wind speed (maximum)	215 km/h (115 knots)	185 km/h (100 knots)
Rainfall near lagoon (landfall day)	160 mm	80 mm
Central pressure (minimum)	940 hPa	950 hPa
Pressure drop (maximum)	66 hPa	54 hPa
Storm surge (maximum)	2–2.5 m above astronomical tides	1.4 m above astronomical tides
Economic impact	USD $696 million	USD $3.4 billion
Total number of fatalities	45	124

The data were collected from reports of central and state government organisation (IMD 2013, 2014; GoO 2013)

extracted from 27 locations (P1-P27) marked in Fig. 1e using MOD09GQ data. Nine locations from each sector; NS (P1-P9), CS (P10-P18) and SS (P19-P27) were randomly selected to extract the TSS and Chl-*a* concentration in the lagoon pre- and post-VSCSs. The following polynomial equation was used to extract the TSS concentration from MODIS products:

$$\text{TSS}_{\text{Polynomial}} = 13,181 \times R_{\text{rs}} \ (\text{MODIS B1})^2 - 1408.6 \times R_{\text{rs}}(\text{MODIS B1}) + 44.15 \quad (1)$$

The above TSS model (Eq.1) was developed for Chilika Lagoon by Kumar et al. (2016) by re-parameterising Miller and McKee's linear TSS model (Miller and McKee 2004). The wide range of in situ TSS samples (1.2 to 161.7 mg/L) from different months and years were used in re-parameterising the Miller and McKee's TSS model. The calibration result revealed a significant relationship between TSS and the R_{rs} ($R^2 = 0.91$; $n = 54$; $p < 0.001$). In addition to an independent validation (RMSE = 2.64 mg/L; $n = 16$) at Chilika Lagoon, the model was also validated for different geographic locations (Taihu Lake, China; Poyang Lake, China; La-plata River Estuary, Argentina; Mobile Bay Estuary, USA) to test its broad geographic applicability (more detail can be found in Kumar et al. 2016).

Spatio-temporal Chl-*a* mapping was carried out using the recently published slope model (Eq. 2) for Chilika Lagoon

(Srichandan et al. 2015b). This model was developed with the in situ Chl-*a* samples corresponding to the cyclone month (October 2013). A significant relationship ($R^2 = 0.59$; $n = 29$; $p < 0.001$; RMSE = 20.7 %; bias = 8.4 %) was established between in situ Chl-*a* concentration and slope of MODIS band 3 and band 4 as follows:

$$\text{Chl}-a = 211.98 \times \exp(6320.3 \times \text{slope reflectance}) \quad (2)$$

where,

$$\text{Slope reflectance} = \frac{R_{\text{rs}} \ (\text{B3}) - R_{\text{rs}} \ (\text{B4})}{\left| \text{Band center(B3)} - \text{Band center (B4)} \right|} \quad (3)$$

$$\text{Reflectance (band 3)} = 0.4796 \times \text{reflectance (band 1)} + 0.0189 \quad (4)$$

$$\text{Reflectance (band 4)} = 0.7186 \times \text{reflectance (band 1)} + 0.0407 \quad (5)$$

A similar slope model was used to derive Chl-*a* concentration from MODIS data from Lake Pontchartrain, Louisiana, USA (Mishra and Mishra 2010). Accuracy was a major factor for selecting the previously published TSS and Chl-*a* models because both were calibrated and validated with in situ samples from Chilika Lagoon itself. The accuracy of Chl-*a* model

implemented in this study was compared with four other published models (Gitelson et al. 2003; Kahru et al. 2004; Zhang et al. 2011; El-Alem et al. 2012), and it was found to perform better compared with others (more details can be found in Srichandan et al. 2015b).

Giovanni-Based TRMM and GLDAS Products

The limited field-based observation of environmental factors during cyclonic events invoked the need of satellite sensors and model-derived products. NASA's Giovanni system facilitates access to a range of remote sensing data and other earth science data sets, which helps researchers to implement selected data to a broad area of research field such as terrestrial, atmospheric and marine environment (Acker et al. 2014). It includes data from various NASA missions and projects. Tropical rainfall measuring mission (TRMM) precipitation products used in this study were downloaded using the Giovanni web based application tool TRMM Online Visualization and Analysis System (TOVAS) (http://disc.sci.gsfc.nasa.gov/precipitation/tovas/). There are different TRMM products which can be visualised and downloaded using TOVAS which is in operation since March 2001. These products include: (1) 3-h TRMM and other satellite rainfall (3B2RT) data from January 2002 to present; (2) TRMM level-3 daily rainfall (3B42) from January 1998 to present; (3) TRMM level-3 monthly rainfall (3B43) from January 1998 to present (Leptoukh et al. 2005). In this study, 3-h precipitation products (TRMM_3B42RT.007) were used in order to capture the highest rainfall event around the lagoon catchment on the landfall day of the two VSCSs (*Phailin* and *Hudhud*). TRMM data from Giovanni was also used by Acker and Leptoukh (2007) to show the rainfall accumulation during Hurricane *Ivan* (16 September 2004) around Gulf of Mexico, Florida and Alabama.

In addition to TOVAS, Global Land Data Analysis System (GLDAS) was also used for visualising the GLDAS-derived rainfall rate, surface runoff and near-surface wind speed products in order to capture the surface level alteration, especially for analysing the variability in the catchment of the lagoon, caused by the anniversary cyclones. GLDAS is an interactive programme which incorporates both satellite and ground based observations at a spatial resolution of $0.25 \times 0.25°$ (Fox and Rowntree 2013). Rodell and Houser (2004) and Fang et al. (2008) have described about GLDAS products in detail in their studies. In this study, the 3-hly product (GLDAS_NOAH025SUBP_3H.001) and monthly product (GLDAS_NOAH025_M.001) were used for analysing the short- and long-term variations in physical (surface runoff: kg/m^2 s^{-1}) and meteorological (rainfall rate: kg/m^2 s^{-1} and wind speed: m/s) parameters. Monthly data were time averaged to produce annual averaged data and three-hourly data were time averaged to generate 1-day averaged data. These

products are based on NOAH model (http://disc.sci.gsfc.nasa.gov/datacollection/GLDAS_NOAH025_3H_V020.shtml). NOAH model incorporate near surface atmospheric forcing data as input such as soil moisture, soil temperature, canopy water content, energy flux and water flux terms of surface energy balance and water energy balance for simulation. All data were visualised with Giovanni tool and the corresponding NetCDF files were downloaded for each transect for further extraction and analysis.

Differential Impact Analysis

MODIS true colour images corresponding to pre-VSCSs (7 October 2013 and 2014: the nearest cloud-free image before the landfall of cyclones), landfall day (12 October 2013 and 2014) and post-VSCSs (14 October 2013 and 2014) were incorporated to show the differential change in water colour of the Chilika Lagoon and its surrounding region. However, MODIS 1-day revisit period limited its applicability for tracking the duration and path of cyclone on an hourly basis. Thus, we incorporated Giovanni-derived three-hourly rainfall and surface runoff transects on landfall day to show the track, duration and the maximum area of impact caused by both VSCSs. In addition, monthly and annual transects derived from Giovanni were also incorporated for comparing the short-term cyclone impact with normal environmental conditions.

Data extracted from Giovanni transects corresponding to surface wind speed, rainfall rate and surface runoff for the catchment area of the lagoon was compared on a daily basis for the month of October, 2013 and 2014. Each of the 3-h products were time averaged for 24 h using Giovanni's time-averaged map tool (http://giovanni.sci.gsfc.nasa.gov/giovanni/), and the averaged transect files were downloaded in NetCDF format. The units of surface runoff and rainfall rate were converted from kilogrammes per square metre per second to grammes per square metre per hour using a multiplication factor of 3,600,000 in SeaDAS statistical tool. Further, a geometrical mask was used to extract the time averaged data corresponding to the catchment area of the lagoon. There were three geometrical masks used for extracting the data from different catchments (northern catchment (NC), western catchment (WC) and overall catchment) of the lagoon (Fig. 4a). The first geometrical mask corresponding to NC covered 15 grid cells of $0.2° \times 0.2°$ ($\approx$7408 km^2) geographical area (19.9° S–20.4° N, 84.6° W–85.8° E). The second geometrical mask corresponding to WC covered eight grid cells of $0.2° \times 0.2°$ ($\approx$3952 km^2) geographical area (19.4° S–19.9° N, 84.6° W–85.2° E). The third geometrical mask corresponding to overall catchment covered 23 grid cells of $0.2° \times 0.2°$ ($\approx$11,360 km^2) geographical area (19.4° S–20.4° N, 84.6° W–85.8° E). In addition to date-wise comparison of these physical and meteorological variables, the

correlation analysis of surface runoff (one of the major factors that is known to increase turbidity in the water column for this area (Kumar et al. 2016) with rainfall rate and wind speed was carried out. Moreover, the annual average rainfall rate and annual average surface runoff were also compared with mean rainfall rate and surface runoff data corresponding to cyclone months and landfall day to evaluate the extent of impact caused by both VSCSs.

The ultimate objective of this study was to evaluate the differential impacts of VSCSs on the biophysical parameters that govern the water quality of the lagoon. In order to accomplish the objective, sector-wise mean TSS and mean Chl-a data from 27 locations marked in Fig. 1e (nine from each sector) were incorporated in comparative analysis for the cyclone months (October 2013 and 2014) in both years. In addition to cyclone months, previous 12 years' (2001–2012) MODIS data were investigated for the post-landfall date (October 14) that captured the maximum impact of VSCSs. However, only few years had cloud-free data available for that date and those were included in the comparative analysis of the above biophysical parameters. Moreover, TSS and Chl-a maps were created and placed side by side to demarcate the spatio-temporal variation in these parameters pre- during post-VSCS periods. Sector-wise correlation analysis was also carried out between the two parameters (TSS and Chl-a) using the data corresponding to entire cyclone months.

Results

MODIS true colour images prior to both VSCSs indicated the usual turbidity regime of the lagoon as found by Kumar et al. (2016), i.e. high turbidity in NS due to heavy freshwater influx and comparatively low turbidity in CS and SS (Fig. 2a, b). One important difference observed in true colour images was that prior to *Phailin*, land pixels of the MODIS image appeared darker compared with pre-*Hudhud* (Fig. 2a, b). Also, the BOB appeared more turbid (light blue) in pre-*Phailin* MODIS image (Fig. 2a) compared with the pre-*Hudhud* image (dark blue) (Fig. 2b). The reason behind this difference is most likely the ~3-fold high rainfall during the beginning of October 2013 (1st week total precipitation, 1.46 kg/m² for overall catchment 19.4° N–20.4° N and 84.6° E–85.8° E) compared with initial period of October 2014 (1st week total precipitation, 0.55 kg/m² for the same catchment) which made the land surface saturated and appeared darker and also increased runoff to BOB making it more turbid. The landfall day image of VSCS *Phailin* revealed that its swath covered the entire Chilika Lagoon and its eye was clearly demarcated close to the lagoon (Fig. 2c). On the other hand, the outer band of VSCS *Hudhud* covered the Chilika Lagoon and its eye was comparatively at a larger distance from the lagoon (Fig. 2d). Chilika Lagoon appeared completely turbid (brown colour) in

post-*Phailin* MODIS image and a large sediment plume is also apparent that extended towards the BOB due to flooded river extracts (Fig. 2e). The flood intensity in Rushikuliya River below the Chilika Lagoon can be observed easily in MODIS images post-*Phailin* (Fig. 2e). In contrast, the post-*Hudhud* MODIS images revealed lesser impact on Chilika Lagoon in terms of turbidity levels, particularly in CS and SS, based on the visual analysis of the water colour in MODIS true colour data. Also, the spatial extent of the sediment plumes in BOB appeared a little thinner most likely due to comparatively lesser river discharge (Fig. 2f).

The path of both VSCSs and how long their impact lasted around the Chilika Lagoon can be observed in the three-hourly Giovanni-derived TRMM transects (Fig. 3). There was continuous rainfall observed over or near Chilika Lagoon (indicated by open circles in Fig. 3a–h) for 24 h on the landfall day of *Phailin*. In contrast, transects corresponding to landfall day of *Hudhud* revealed that the precipitation over or near the lagoon lasted only for 9–12 h (Fig. 3i–p). Swath of both the VSCSs and their progress can be observed in these transects. The landfall points of *Phailin* (Gopalpur) and *Hudhud* (Visakhapatnam) are shown by dashed arrows with respect to Chilika Lagoon (solid arrow) (Fig. 3g, l). The 24-h analysis revealed very high average rainfall (~100–110 mm) near the lagoon during *Phailin* compared with *Hudhud* (~55–60 mm).

The precise effect of heavy rainfall around Chilika Lagoon is further revealed by the three-hourly surface precipitation and surface runoff transects (Fig. 4). Three-hourly surface runoff transects showed a close temporal matching with high rainfall locations (Fig. 4a–p). As suspected, the 24 h comparative result shown in Fig. 4q, r indicated high surface runoff during *Phailin* (NC: highest up to 4379.45 g/m² h⁻¹; WC: highest up to 683.25 g/m² h⁻¹) due to high precipitation (NC: highest up to 17,076.28 g/m² h⁻¹; WC: highest up to 9198.02 g/m² h⁻¹) in contrast to relatively lower surface runoff on the landfall day of *Hudhud* (NC: highest up to 532.48 g/ m² h⁻¹; WC: highest up to 253.41 g/m² h⁻¹) due to comparatively less precipitation (NC: highest up to 5279.74 g/m² h⁻¹; WC: highest up to 4852.47 g/m² h⁻¹) and passage of *Hudhud* from sector with lesser tributaries and more vegetated areas.

The surface runoff transects in both cases indicated that the maximum contribution was from northern and north-western zone (together considered NC), where the lagoon receives highest surface runoff due to the heavy discharge from rivers and distributaries, compared with WC (Kumar et al. 2016) (Fig. 4; also refer to Fig. 2a, b). The surface runoff transects revealed a significant increase in magnitude (~1 order of magnitude increase) after 12:00 p.m. on the landfall day of *Phailin*, and it persisted for continuous 9 h (Fig. 4(e'–g', r)). In contrast, there was no such order difference observed during VSCS *Hudhud* in the magnitude of surface runoff (Fig. 4 (i–p, r)). The above results were primarily from the landfall
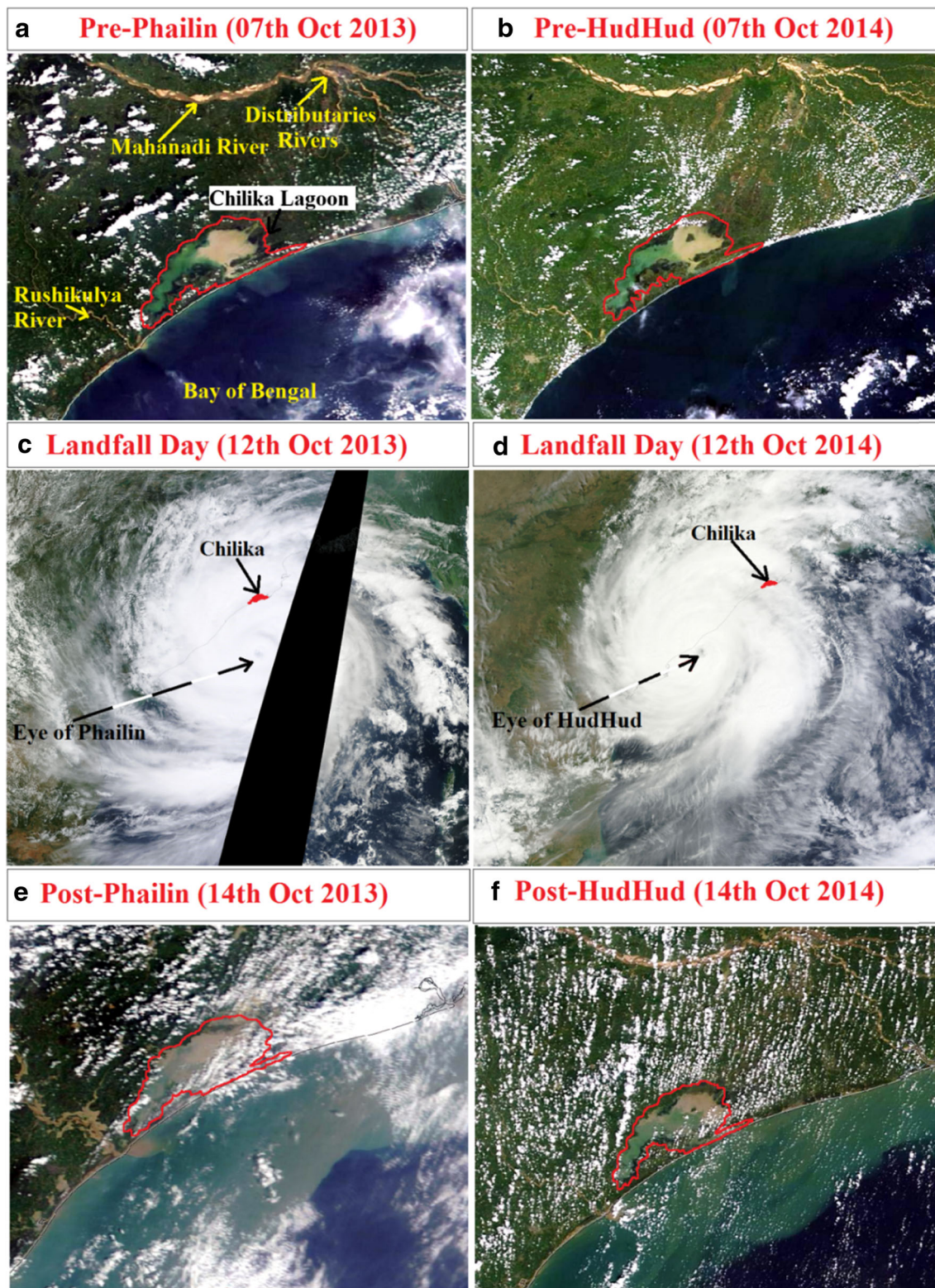
Fig. 2 Visual analysis of the impacts of VSCSs *Phailin* and *Hudhud* on Chilika Lagoon and surrounding region using MODIS true colour images: pre-*Phailin* (**a**), pre-*Hudhud* (**b**), landfall day of *Phailin* (**c**), landfall day of *Hudhud* (**d**), post-*Phailin* (**e**) and post-*Hudhud* (**f**). Chilika Lagoon is demarcated by the *red polygon*, and the distributaries of Mahanadi River (major source of freshwater for the lagoon) connecting the lagoon are marked by *solid arrow* (**a**). The eyes of both cyclones are indicated by *dashed arrow* (**c**, **d**)

Rainfall Rate (Phailin-2013)
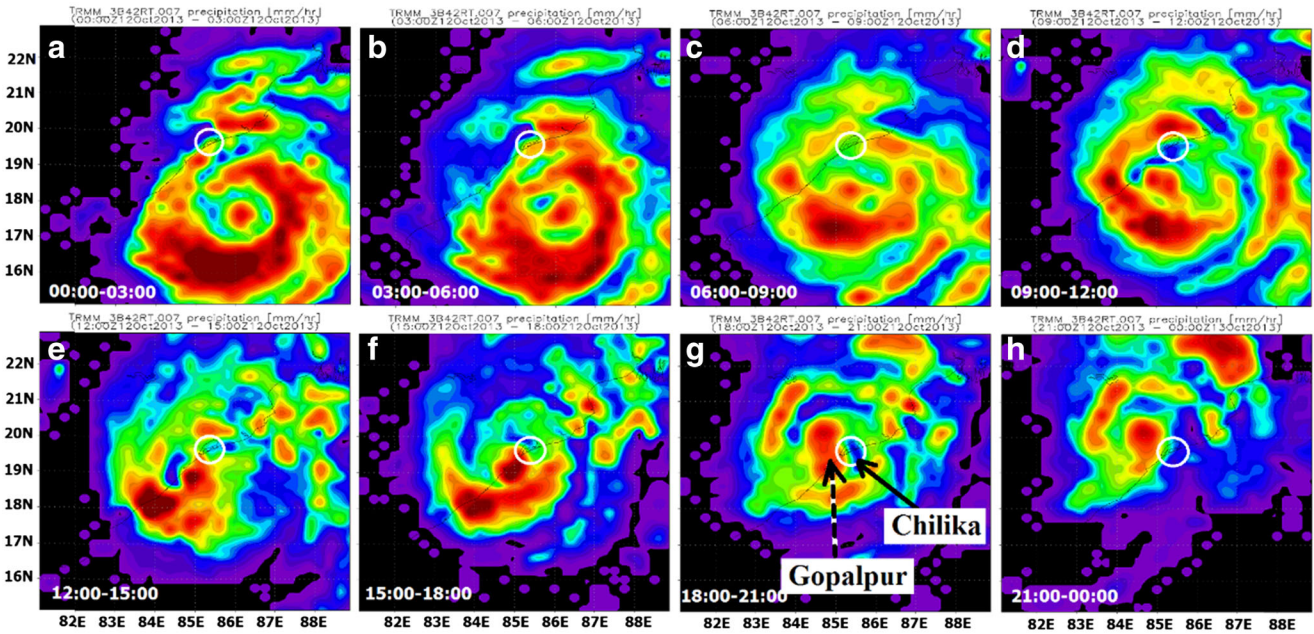
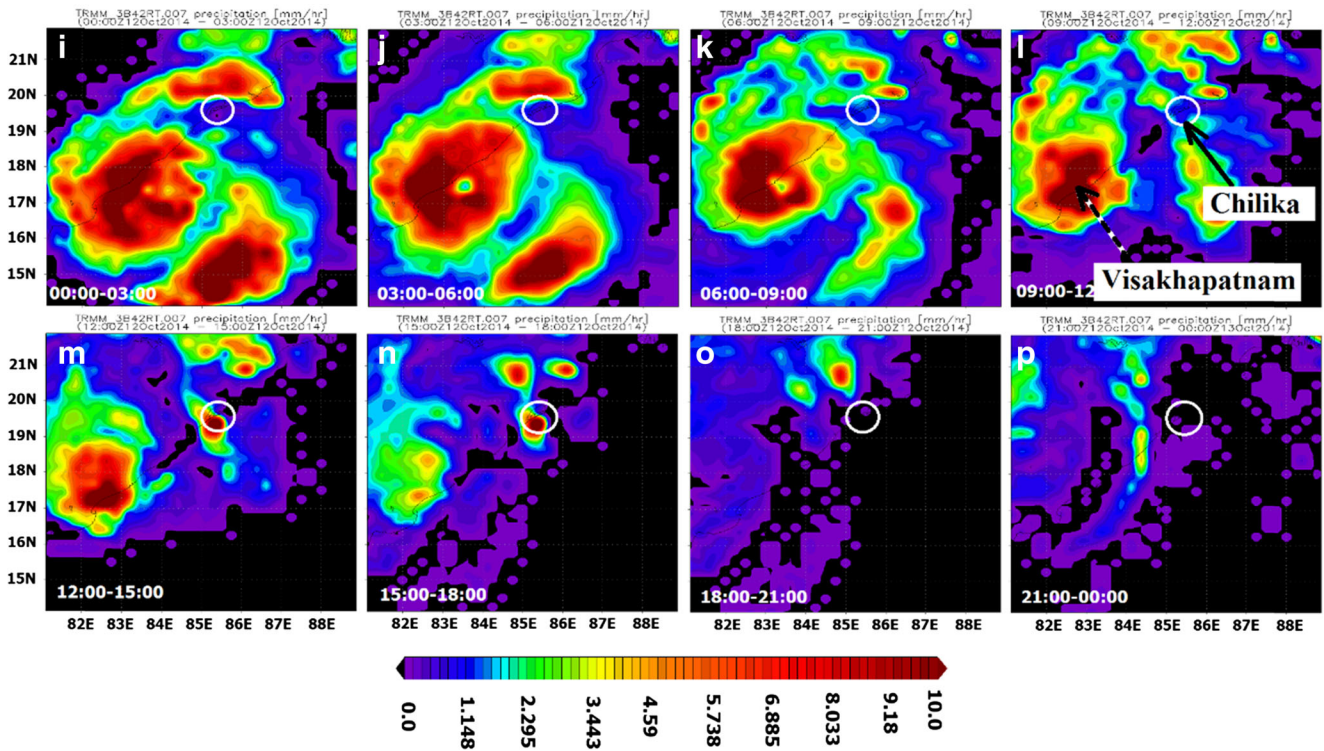## Rainfall Rate (HudHud-2014)

Fig. 3 Precipitation map produced by Giovanni web based application tool using TRMM three-hourly product for 24 h on the landfall day of *Phailin* (12 October 2013) and *Hudhud* (12 October 2014). Chilika Lagoon is indicated by *solid arrows with open circle*, and the landfall points are indicated by *dashed arrows* (**g**, **l**)

day of both VSCSs. In order to quantify the variability of these parameters under normal environmental conditions, both pre- and post-cyclone data corresponding to entire month of October 2013 and 2014 were analysed. Also, an additional variable, near surface wind speed was incorporated in further analysis.

Figure 5 shows the variability in mean surface wind speed, mean rainfall rate (surface precipitation) and mean surface
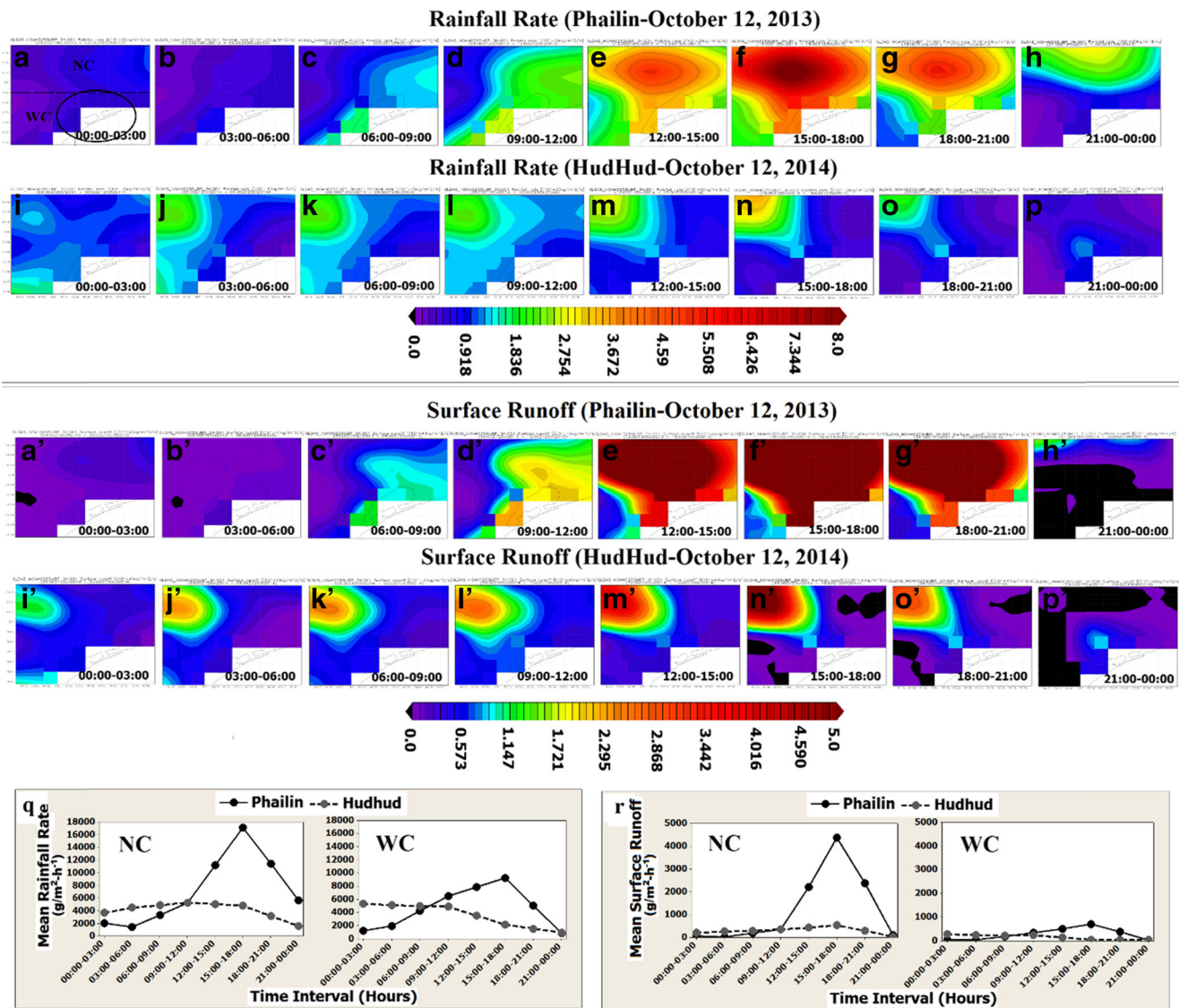
Fig. 4 Rainfall rate (*a–p*) and surface runoff (*a'–p'*) map produced by Giovanni Web-based application tool using GLDAS three-hourly products for 24 h on the landfall day of *Phailin* (12 October 2013) and *Hudhud* (12 October 2014) near the catchment area. The two catchments northern (*NC*; 19.9° S–20.4° N; 84.6° W–85.8° E) and western (*WC*; 19.4° W–19.9° N; 84.6° W–85.2° E) used in comparative analysis are demarcated by *dashed lines*, and Chilika Lagoon is marked with *open circle* (*a*). Catchment-wise comparison of rainfall rate (*q*) and surface runoff at every 3 h (*r*)

runoff for overall catchment corresponding to the entire month before-during-after the cyclones (October 2013 and 2014). The gradual increase in surface wind speed started on 9 October 2013 (9.82 km/h) and reached to peak level on the landfall day of *Phailin* (12 October 2013: 53.72 km/h) (Fig. 5a). Similar increase in surface wind speed started on 7 October 2014 (7.18 km/h) and continued to increase till the landfall day of *Hudhud* when it reached at its peak level (12 October 2014, 35.55 km/h). The wind speed magnitude on the landfall day was 51 % higher for *Phailin* compared with *Hudhud* (Table 2). Unlike wind speed, the rainfall rate and surface runoff which are highly correlated (R^2 = 0.89 and 0.96) increased at an exponential rate on the landfall day and decreased at the same rate after the passage of the cyclones.

High sustained wind and runoff may have triggered the re-suspension of bottom sediments which increased the turbidity in the lagoon drastically on the landfall day of *Phailin* (Table 2). An earlier study based on field measurement of turbidity in the lagoon has shown that before *Phailin* the turbidity of the lagoon was 32.8 NTU which increased to 60.4 NTU after *Phailin* (Srichandan et al. 2015b). In contrast, comparatively lower mean surface runoff (243.97 g/m^2 h^{-1}) due to lower mean surface precipitation (3809.33 g/m^2 h^{-1}) and lower wind speed on the landfall day of *Hudhud* was not able to increase the turbidity of the lagoon to *Phailin* level (Table 2) (Fig. 2f). The catchment-wise analysis revealed that though there was a significant difference between the cyclones' monthly mean surface wind speed (NC, 37.58 % and

Fig. 5 Variation in
meteorological parameters: mean
surface wind speed and mean
rainfall rate (**a**, **b**) and physical
parameter: mean surface runoff
(**c**) corresponding to overall
catchment (19.4° N–20.4° N and
84.6° E–85.8° E) surrounding the
Chilika Lagoon for October (*x*-
axis: days of October 2013 and
2014; *y*-axis: mean surface runoff,
mean rainfall rate and mean
surface wind speed). The *open
circles* and *boxes* indicated the
unprecedented level of magnitude
on the landfall day for both
VSCSs, *Phailin* (12 October
2013) and *Hudhud* (12 October
014), respectively
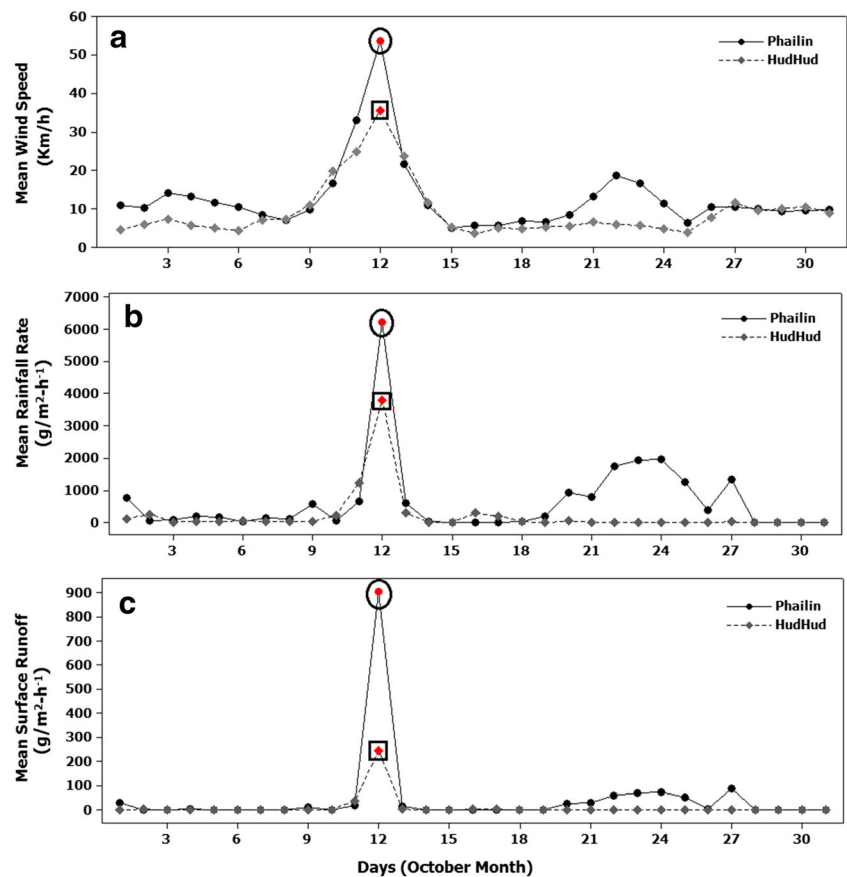
WC, 36.29 %) and monthly mean rainfall rate (NC, 192.54 %
and WC, 210.96 %), the changes were similar for both catch-
ments (Table 2). However, substantial difference in monthly
mean surface runoff was found between the two catchments

(NC, 387.26 % and WC, 254.36 %) (Table 2). Comparison
between the cyclones' mean surface runoff on landfall day
revealed significant differences between two catchments as
well (NC, 300.08 % and WC, 63.03 %).

Table 2 Catchment-wise
comparison between physical and
meteorological parameters for the
entire October and landfall day
for both cyclones (overall
catchment (OC), northern
catchment (NC) and western
catchment (WC))

Parameters	October—entire month			Landfall day		
	Phailin (October 2013)	Hudhud (October 2014)	% higher (Phailin)	Phailin 12 October 2013	Hudhud 12 October 2014	% higher (Phailin)
Mean surface wind speed (km/h)						
OC	12.79	9.33	+37.08	53.72	35.55	+51.11
NC	14.13	10.27	+37.58	60.33	38.08	+58.42
WC	11.19	8.21	+36.29	45.79	32.51	+40.84
Mean rainfall rate (g/m² h⁻¹)						
OC	658.12	222.03	+196.41	6235.21	3809.33	+63.68
NC	656.30	224.34	+192.54	6817.69	3900.47	+74.79
WC	664.66	213.74	+210.96	4138.22	3481.22	+18.87
Mean surface runoff (g/m² h⁻¹)						
OC	44.71	9.6	+365.72	904.16	243.97	+270.61
NC	50.14	10.29	+387.26	1092.14	272.98	+300.08
WC	25.16	7.1	+254.36	227.43	139.5	+63.03

The catchment-wise correlation also supported the above findings with much higher slope for NC compared with WC for both cyclones, *Phailin* and *Hudhud*. The trend line slope between mean surface runoff and mean rainfall rate for NC was found to be ~3× higher than WC during *Phailin* (NC, 0.1466 and WC, 0.04628) and 1.7× higher during *Hudhud* (NC, 0.06758 and WC, 0.03944) (Fig. 6a, b). It also indicated much higher surface runoff from northern side during the cyclonic events. Correlation between mean surface runoff and mean surface wind speed resulted in much higher slope for NC, i.e. ~4× higher than WC (NC, 15.29 and WC, 4.298) during *Phailin* suggesting strong impact of wind in NC compared with WC in driving the surface runoff (Fig. 6c). However, no significant difference in slope between the catchments was observed during *Hudhud* (NC, 4.378 and WC, 3.443) (Fig. 6d). The correlation results presented above include the data from the landfall day which appeared to be an outlier because of extremely high precipitation, surface runoff and wind speed on that day (Fig. 6a–d). However, all correlation results, including and excluding the landfall day for both catchments, were found to be statistically significant ($p < 0.001$), except correlation between wind speed and surface runoff, where exclusion of the landfall day data made the relationship between the two parameters insignificant. It suggested that low to moderate wind speed alone is not sufficient to drive the surface runoff, and a combination of meteorological (mainly rainfall) and physical factors is required (http://water.usgs.gov/edu/watercyclerunoff.html), which was present on the landfall day of both cyclonic events. In other words, relatively low wind speed does not influence surface runoff that much, however, extremely high wind speed does and that is the reason why the relationship between wind speed and surface runoff turned significant when the landfall day values were incorporated in the analysis. On the contrary, precipitation alone is the dominant factor among all parameters which controls the surface runoff (even with the exclusion of the landfall day data) and the same was evident from transects which showed close match up of high precipitation locations with high surface runoff areas (Figs. 4 and 7).

In order to compare the short-term variation in rainfall and runoff with the annual and the entire month of October, monthly transects were time averaged and visualised using Giovanni Web-based interactive tool (Fig. 7). The time-averaged data
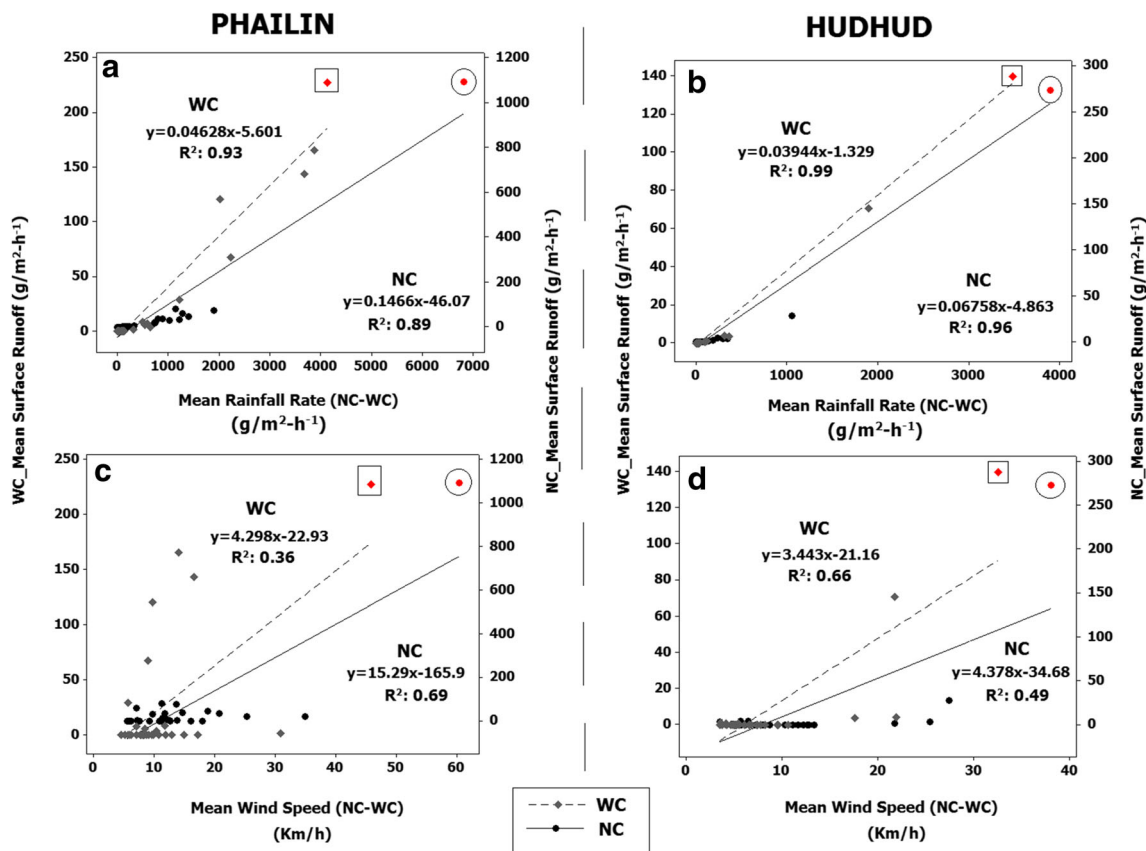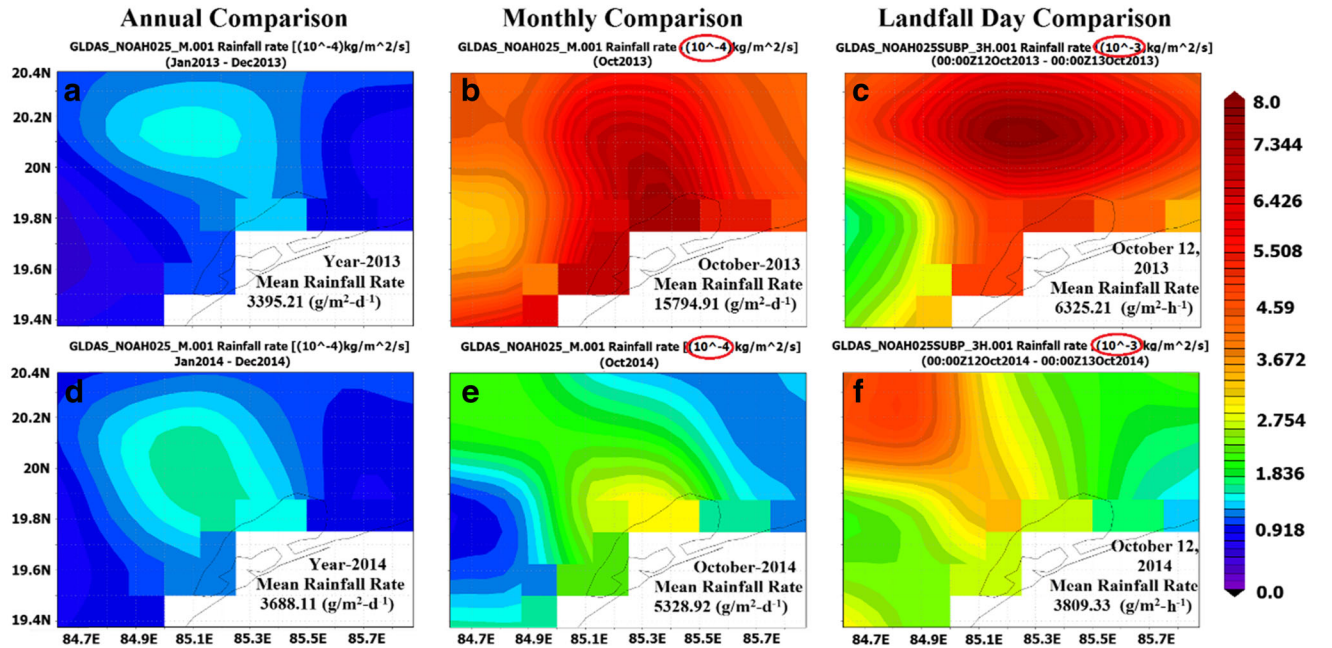

Fig. 6 Correlation between time averaged daily surface runoff and rainfall rate for cyclone months: October 2013: *Phailin* (**a**), October 2014: *Hudhud* (**b**). Averaged surface runoff was correlated with time-averaged near-surface wind speed for both cyclone periods: *Phailin* (**c**) and *Hudhud* (**d**). The primary *y*-axis represents WC data (*dashed line*) and secondary *y*-axis represents NC data (*solid line*). *x*-axis represents both NC and WC data. *Circles* and *boxes* are used for highlighting the significantly large value of surface runoff on the landfall day of *Phailin* and *Hudhud*, respectively. All the correlation results were found to be statistically significant ($p < 0.001$)
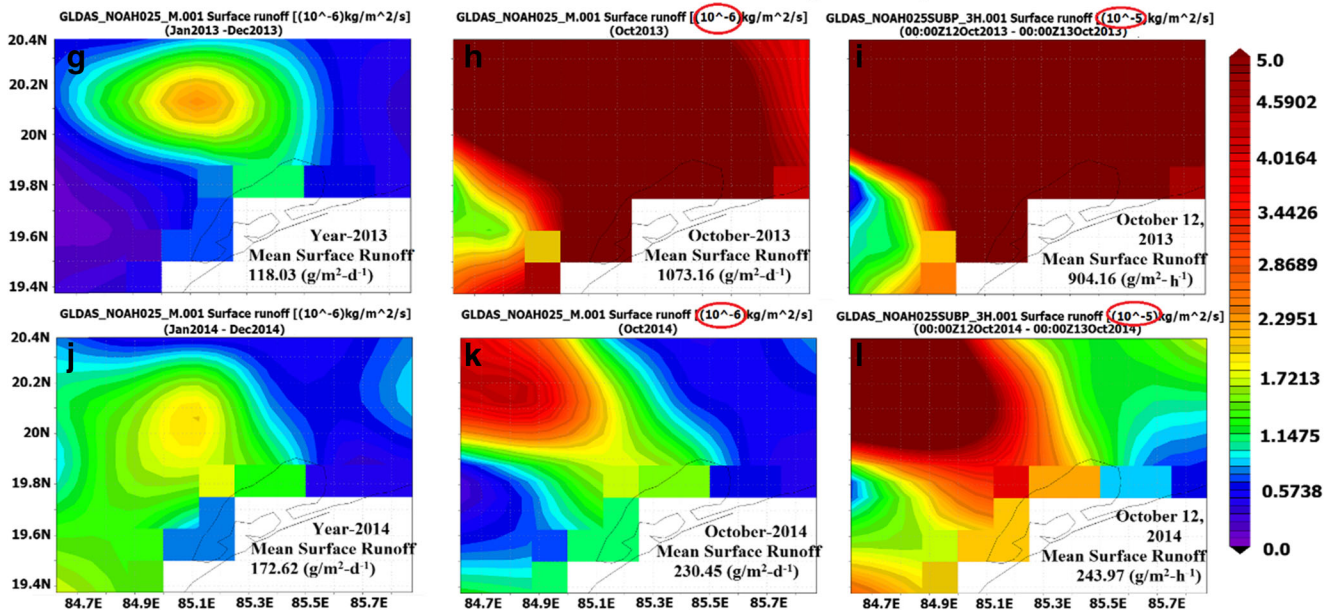
Rainfall Rate (Comparison)

Fig. 7 Comparison of rainfall and runoff on an annual, monthly (October) and daily basis (landfall day) for VSCSs *Phailin* and *Hudhud*. Annual rainfall: 2013 (**a**) and 2014 (**d**); annual runoff: 2013 (**g**) and 2014 (**j**); October month rainfall: 2013 (**b**) and 2014 (**e**); October month runoff: 2013 (**h**) and 2014 (**k**); landfall day rainfall: 2013 (**c**) and 2014 (**f**); landfall day runoff: 2013 (**i**) and 2014 (**l**). The order difference in annual mean and monthly mean magnitude (10^{-4} to 10^{-3} kg/m^2 s^{-1} in rainfall and 10^{-6} to 10^{-5} kg/m^2 s^{-1} in runoff) with respect to landfall day is demarcated in *circles*

were extracted for the overall catchment area (19.4° N–20.4° N and 84.6° E–85.8° E) previously used for the analysis of landfall day and cyclone month (October). It was observed that during VSCS *Phailin*, the total rainfall in October 2013 was 15,794.91 g/m^2 day^{-1} ($\approx$489.64 kg/m^2 for the entire month) which alone contributed 39.5 % to the total mean annual rainfall (1239.25 kg/m^2) in 2013 (Table 3). In addition, on the landfall day of *Phailin*, the total rainfall was 149.64 kg/m^2, approximately 30.56 % of the total rainfall (489.64 kg/m^2) in October 2013. This heavy rainfall led to high surface runoff on landfall day (21.69 kg/m^2) which accounted for 65.22 % of total surface runoff (33.26 kg/m^2) during October 2013 (Table 3). Also, runoff triggered by VSCS *Phailin* contributed about 77.22 % (33.26 kg/m^2) to the total mean annual runoff

Table 3 Comparative rainfall rate and surface runoff data for two different years (2013 and 2014) corresponding to anniversary cyclones *Phailin* and *Hudhud*

Parameters	Average annual		October		Landfall day	
	Rate (g/m^2 day^{-1})	Total (kg/m^2)	Rate (g/m^2 day^{-1})	Total (kg/m^2)	Rate (g/m^2 h^{-1})	Total (kg/m^2)
Rainfall rate						
Phailin (2013)	3395.21	1239.25	15,794.91	489.64	6235.21	149.64
Hudhud (2014)	3688.11	1346.16	5328.92	165.19	3809.33	91.42
Surface runoff						
Phailin (2013)	118.03	43.08	1073.16	33.26	904.16	21.69
Hudhud (2014)	172.62	63.01	230.45	7.14	243.97	5.85

(43.08 kg/m^2) of 2013 (Table 3). The results indicated that during *Phailin*, the entire month was affected by heavy rainfall even before the VSCS. On the contrary, during VSCS *Hudhud*, only the landfall day showed large increases in these factors, not for the entire month. The total rainfall during October, 2014 was only 12.27 % (165.19 kg/m^2) of the total mean annual rainfall (1346.16 kg/m^2) that led to the lower mean surface runoff of 7.14 kg/m^2 which was only 11.33 % of mean annual surface runoff (63.03 kg/m^2) compared with the previous year (Table 3). However, on the landfall day of *Hudhud*, the mean rainfall accounted for 55.34 % (91.42 kg/m^2) of the entire month's mean rainfall budget (165.19 kg/m^2). A substantial increase in surface runoff was also noticed on the landfall day of *Hudhud* due to heavy rainfall, accounting up to 81.93 % (5.85 kg/m^2) of the monthly average surface runoff in October 2014 (7.14 kg/m^2).

The mean TSS concentration was found to be significantly higher in NS (*Phailin*, 131.36 mg/L; *Hudhud*, 75.13 mg/L) and CS (*Phailin*, 35.32 mg/L; *Hudhud*, 13.53 mg/L) October 2013 (*Phailin* month) compared with October 2014 (*Hudhud* month) (Fig. 8; Table 4). The mean TSS in SS was observed to be very similar in magnitude between October 2013 (16.24 mg/L) and 2014 (15.33 mg/L) and lowest among all sectors (Fig. 8; Table 4). In contrast, the mean Chl-*a* concentration was found to be relatively higher for the month of *Hudhud* compared with *Phailin* in all the sectors (*Phailin*: NS, 4.21 µg/L; CS, 11.36 µg/L; SS, 21.94 µg/L; *Hudhud*: NS, 6.93 µg/L; CS, 18.44 µg/L; SS, 24.61 µg/L) of the lagoon (Fig. 8; Table 4).

In order to demonstrate the relative magnitude difference on the landfall day compared with the rest of the month, MODIS-based model-derived mean TSS and mean Chl-*a* values are plotted for October, 2013 and 2014 using all cloud-free data (Fig. 8a–d; Table 5). Figure 8e, f shows the annual variability in TSS and Chl-*a* from 2001 to 2014 in October just a day after the cyclone to visualise the impact compared with normal years. Overall, the sector-wise variability and the inverse relationship between TSS and Chl-*a* is clearly distinguishable. Chilika lagoon is known to have a clear historical turbidity gradient, highest in NS, moderate in CS and least in SS (Kumar et al. 2016), which is somewhat disturbed after the passage of the cyclones. Similarly, the Chl-*a* gradient in the lagoon was exactly opposite to the turbidity gradient with SS consistently showing higher values compared with CS and NS. The magnitude difference in the gradient is appeared to be disturbed as well. Table 5 revealed a significant increase in TSS in all sectors (NS, 154 %; CS, 148 %; SS, 107 %) of the lagoon from pre-*Phailin* to post-*Phailin* stage and a decrease in Chl-*a* concentration in all sectors (NS, −61 %; CS, −63 %; SS, −67 %) after the landfall of *Phailin* (Fig. 8). However, post-*Hudhud* mean TSS data indicated an increase in CS (157 %) and SS (26 %) and surprisingly a decrease in NS (−3 %) might have favoured the Chl-*a* concentration increase in NS (+35 %) of the lagoon (Table 5). Mean Chl-*a* concentration in CS and SS reduced (CS: −51 %; SS: −26 %) post-*Hudhud* while TSS increased in these two sectors. Comparative results revealed that post-*Phailin* TSS was significantly higher in all the sectors (NS, 228 % higher; CS, 142 % higher; SS, 160 % higher) compared with post-*Hudhud* TSS (Table 5). In contrast, post-*Phailin* Chl-*a* concentration was found to be lower in all sectors (NS, 75 % lower; CS, 35 % lower; SS, 43 % lower) compared with post-*Hudhud* Chl-*a* (Table 5).

One important difference found from Fig. 8b, d is the lag effect of cyclones on phytoplankton growth in different sectors of the lagoon. It took more than a week after the passage of *Phailin* for the mean Chl-*a* concentration to recover to pre-*Phailin* level comparing the sector-wise values between 7th and 20th October 2013 (7 October 2013—NS, 3.8 µg/L; CS, 13.89 µg/L; SS, 25.62 µg/L and 20 October 2013—NS, 3.41 µg/L; CS, 20.04 µg/L; SS, 28.35 µg/L). However, only 2 days after the passage of *Hudhud*, i.e. on 15 October 2014, the mean Chl-*a* concentration (NS, 8.01 g/L; CS, 21.59 µg/L; SS, 33.31 µg/L) crossed the pre-*Hudhud* level (7 October 2014—NS, 4.46 µg/L; CS, 15.9 µg/L; SS, 20.13 µg/L). In addition to short-term comparison, mean TSS and mean Chl-*a* data were also extracted from 2001 to 2014 using the available cloud-free MODIS images corresponding to 14th October, the day that experienced the maximum impact during both
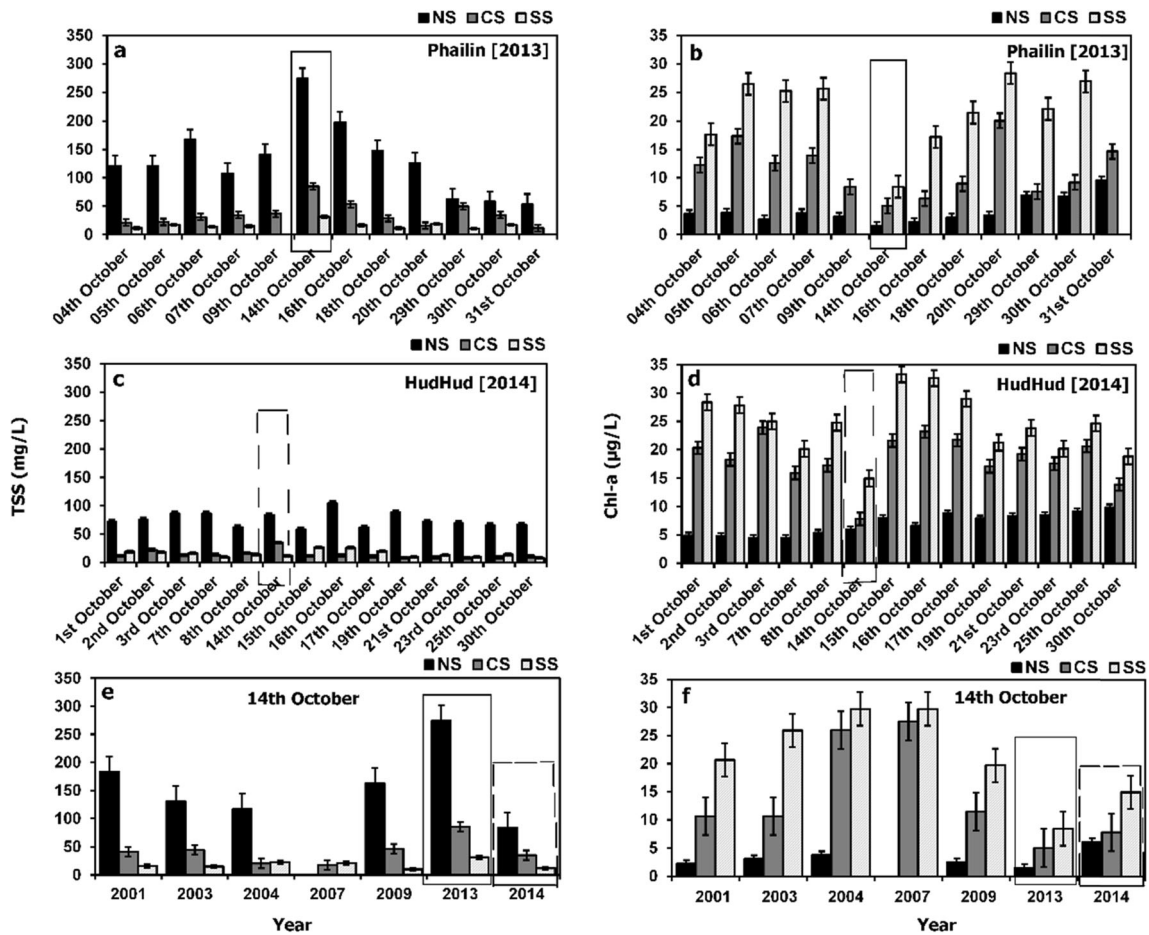
Fig. 8 Variations in mean TSS and mean Chl-*a* concentration across the three sectors of the lagoon (NS, CS, SS). The *bars inside the solid box and dashed box* represent the readings 2 days after the landfall of VSCSs

Phailin and *Hudhud*. TSS and Chl-*a* data was not included from SS of the lagoon on 09 October 2013 and from NS of the lagoon on 14 October 2007 due to cloud cover

VSCSs. Long-term analysis results clearly indicated that the impact of *Phailin* was the highest in terms of both TSS and

Chl-*a* concentration in all the sectors of the lagoon (Fig. 8e, f; Table 5).

Table 4 Sector-wise statistics of TSS and Chl-*a* concentration measured during October (2013 and 2014) for both VSCSs

Parameter	Sector	Cyclone month	Minimum	Maximum	Range	Mean	Standard deviation
Mean TSS (mg/L)	NS	Phailin	53.22	274.05	220.83	131.36	±62.84
		Hudhud	58.05	104.48	46.43	75.13	±13.02
	CS	Phailin	11.61	84.99	73.38	35.32	±19.94
		Hudhud	7.67	35.04	27.37	13.53	±7.26
	SS	Phailin	10.55	31.30	20.75	16.24	±5.97
		Hudhud	7.82	26.99	19.17	15.33	±5.98
Mean Chl-*a* (µg/L)	NS	Phailin	1.48	9.61	8.13	4.21	±2.35
		Hudhud	4.46	9.91	5.45	6.93	±1.78
	CS	Phailin	5.05	20.04	14.99	11.36	±4.56
		Hudhud	7.81	23.91	16.10	18.44	±4.16
	SS	Phailin	8.42	28.35	19.93	21.94	±6.10
		Hudhud	14.93	33.31	18.38	24.61	±5.27

Data were extracted from 27 locations (nine from each sector) and averaged out for each sector to obtain the mean TSS and mean Chl-*a* concentration as presented above

Table 5 Impact on TSS and Chl-*a* concentration derived using MODIS products corresponding to pre-and post-VSCS dates

Parameter	Sector	Pre-Phailin	Post-Phailin	% change (Phailin)	Pre-Hudhud	Post-Hudhud	% change (Hudhud)	Historical (14th Oct)
Mean TSS (mg/L)	NS	107.79	274.05	+154	86.14	83.51	−3	148.27
	CS	34.22	84.99	+148	13.64	35.04	+157	33.96
	SS	14.62	31.30	+107	9.5	12.02	+26	16.75
Mean Chl-*a* (µg/L)	NS	3.80	1.48	−61	4.46	6.01	+35	2.91
	CS	13.89	5.05	−63	15.90	7.81	−51	17.24
	SS	25.62	8.42	−67	20.13	14.93	−26	25.14

7 October 2013 and 2014 data were used as pre-VSCS reference because of the availability of cloud-free data. 14 October 2013 and 2014 MODIS data were used as post-VSCSs. In order to compare with normal years, TSS and Chl-*a* concentration in different sectors of the lagoon, historical mean TSS and mean Chl-*a* data (2001–2014) for 14 October were also included

Impact of anniversary VSCSs on the biophysical parameters of the lagoon was further investigated with the MODIS-derived TSS and Chl-*a* concentration maps and the corresponding true colour images (Fig. 9). The maps were divided into two segments (red dashed line): pre-VSCS (pre-*Phailin* and pre-*Hudhud*) period (left) and post-VSCS period (right) (Fig. 9). Visual analysis of the true colour MODIS images clearly showed the highly turbid NS in all images (Fig. 9). The spatio-temporal pattern of TSS and Chl-*a* concentration pre-VSCS period showed the usual gradients as discussed in the previous sections. There was consistent cloud cover over the lagoon starting from October 9 (2013 and 2014) which limited the availability of cloud-free MODIS images close to the landfall date for both VSCSs. However, just 2 days after *Phailin*, on 14 October 2013, MODIS true colour image (inside the circle: Fig. 9) showed a remarkable increase in turbidity throughout the lagoon and similar pattern was obtained when the TSS model was implemented on MODIS data. On the contrary, Chl-*a* map post-*Phailin* showed a substantial decrease throughout the lagoon on 14 October 2013 (inside the circle: Fig. 9) which could be due to the high TSS concentration that did not allow algal growth (Table 4). The settling of sediment in different sectors can be observed in the images and maps after the landfall of *Phailin* (Fig. 9). From a qualitative standpoint, turbidity started to be diminished on 16 October 2013 in the SS and by 18 October 2013 turbidity in the SS was back to its normal stage (similar to 6 October 2013). Finally, by 20 October 2013, the CS and NS of the lagoon returned to their pre-*Phailin* turbidity level (Fig. 9). On the other hand, post-*Hudhud* TSS maps did not show a significant change in TSS and a gradual increase in Chl-*a* concentration was observed throughout the lagoon (Fig. 9).

In order to study the differential impact of the VSCSs, a 50-km-long transect line was drawn from NS to SS to analyse the gradient of TSS and Chl-*a* (Fig. 10). The goal of the transect analysis was to isolate the loss or disturbance in the gradient, if any, after the VSCSs. The transect plot revealed that the clear-cut TSS gradient existed between NS and CS as observed in Fig. 8 before *Phailin* was somewhat lost due to high runoff and heavy mixing driven by high wind speed. However, post-*Hudhud* transect showed a clear-cut boundary between NS and CS revealing the fact that the cyclone effect was not strong enough to disturb the gradient (Fig. 10a, b). The Chl-*a* transect for *Phailin* did not show much difference between NS and CS because of the intense mixing but revealed a strong gradient between CS and SS. On the contrary, post-*Hudhud* boundary between NS and CS in terms of Chl-*a* magnitude revealed a clear separation with CS experiencing high algal growth than usual.

The correlation between mean TSS and Chl-*a* concentration at nine locations from each sector (marked in Fig. 1e) pre-during post-VSCSs revealed different suspended sediment types dominating in different sectors of the lagoon. The pre-VSCS results indicated a significant inverse correlation between TSS and Chl-*a* concentration in NS and CS of the lagoon (pre-*Phailin*: NS: $R^2 = 0.94$; $p < 0.001$; CS: $R^2 = 0.76$; $p < 0.001$; pre-*Hudhud*: NS: $R^2 = 0.96$; $p < 0.001$; CS: $R^2 = 0.59$; $p = 0.014$) (Fig. 10a–d). In contrast, SS showed a significant positive correlation between TSS and Chl-*a* concentration prior to both *Phailin* ($R^2 = 0.80$; $p < 0.001$) and *Hudhud* ($R^2 = 0.96$; $p < 0.001$) which suggested that this sector's water clarity was primarily determined by phytoplankton compared with NS and CS that were dominated by inorganic and non-living organic sediments (Fig. 10e, f). This finding was similar to Raman et al. (2007) who reported that SS receives maximum contribution of organic nitrogen (82 % of total nitrogen) from its forested catchment and therefore, inorganic matter dominates suspended matter composition in this sector. Results varied for post-*Phailin* compared with post-*Hudhud* in different sectors of the lagoon. The post-*Phailin* correlation indicated negative trend in all sectors of the lagoon due to high TSS concentration (Fig. 10). The NS and CS still showed a significant inverse relationship between mean TSS and mean Chl-*a* concentration (NS: $R^2 = 0.85$; $p < 0.001$ and CS: $R^2 = 0.83$;
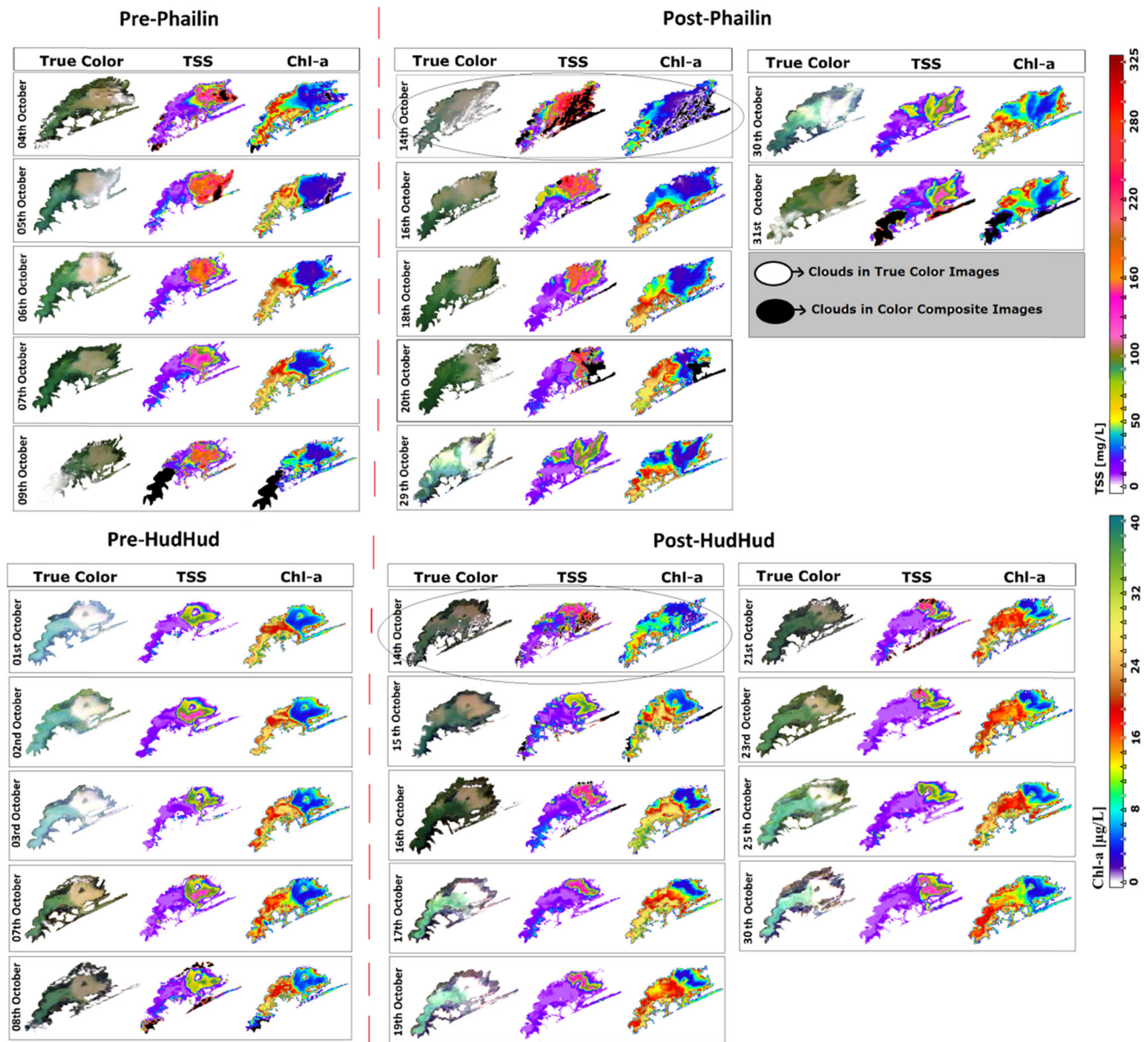
Fig. 9 Spatial and temporal variation of TSS and Chl-*a* concentration in Chilika Lagoon pre-during-post-VSCSs (*Phailin*: October 2013 and *Hudhud*: October 2014) using MODIS true colour images. The images inside the circles show the immediate aftermath of the VSCSs. Gaps observed in the dates are due to the unavailability of cloud-free MODIS products

$p < 0.001$) post-*Phailin* (Fig. 10). Similarly, NS post-*Hudhud* period showed a significant inverse correlation between TSS and Chl-*a* ($R^2 = 0.73$; $p < 0.001$) similar to pre-*Hudhud* but the difference in the magnitude of mean Chl-*a* concentration was three times to that of pre-*Hudhud* period (Fig. 10b). The CS post-*Hudhud* period revealed insignificant correlation ($R^2 = 0.21$; $p = 0.21$) but it showed positive trend in contrast to pre-*Hudhud* period (Fig. 10d). The major difference between the VSCS impact was observed in the SS where post-*Phailin* correlation turned to insignificant compared with pre-*Phailin* significant correlation (Fig. 10e). In contrast, the post-

Hudhud result revealed a significant positive correlation ($R^2 = 0.72$; $p < 0.001$) between mean TSS and mean Chl-*a* concentration for that sector (Fig. 10f).

Discussion

The comparative impact analysis of anniversary cyclones revealed substantial differences in terms of physical, meteorological and biophysical parameters before-during-after their passage over Chilika Lagoon. Also, the economic impact and number of fatalities varied with respect to characteristics
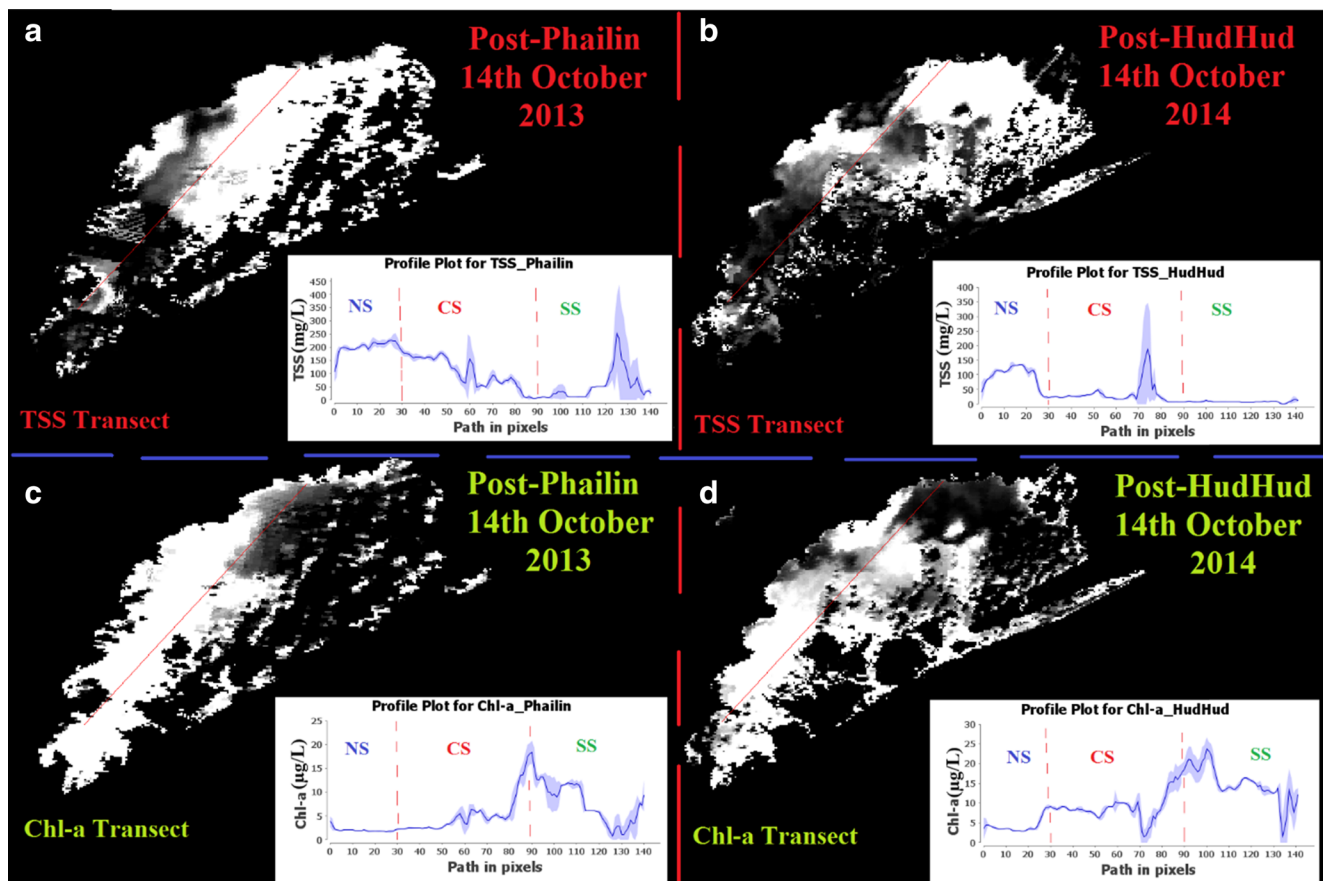
Fig. 10 Spatial variability in biophysical parameters (TSS (**a**, **b**) and Chl-*a* concentration (**c**, **d**)) along a 50-km-long transect (total 140 pixels, 1 pixel = 0.353 km) marked by *solid line* covering all three sectors (NS, CS and SS). The MODIS image used to create the profile was from 14 October 2013 and 2014, the day after the landfall of VSCSs. *x*-axis represents number of pixels (approximation used for number of pixel counts in different sectors: NS = 30; CS = 60; SS = 50) along the transect line, and *y*-axis represents TSS and Chl-*a* concentration for each pixel. The *blue shades* represent standard deviation in TSS and Chl-*a* concentration

of both the cyclones. For example, economic impact and fatalities were higher in case of *Hudhud* as it made landfall near highly urbanised city (Vishakhapatnam) compared with *Phailin* which made landfall near rural area (Gopalpur) and progressed slowly compared with *Hudhud* which moved very rapid. Previous studies also discussed characteristics of a cyclone and associated factors such as landfall location, intensity, trajectory, speed of passage, rainfall and runoff, which can produce significantly different impact (Mallin et al. 2002; Mallin and Corbrett 2006; Srichandan et al. 2015b). However, most of the previous studies discussed only few factors in their results and rest of the factors were theoretically documented (Mallin et al. 2002; Mallin and Corbett 2006; Zhu et al. 2014; Chen et al. 2009; Srichandan et al. 2015b). For instance, study by Zhu et al. (2014) included 12 cyclones but they primarily focused on only one characteristics of cyclone (wind speed) for the associated impact on water quality which assisted the nutrient enrichment and led to phytoplankton bloom. Another study by Chen et al. (2009) which showed the impact of Hurricane *Frances* on water quality of Apalachicola Bay incorporated some more

characteristics of hurricane such as wind speed and wind direction, trajectory and speed of passage but they did not include rainfall, runoff and watershed characteristics. In this study, we documented factors including landfall location, intensity, trajectory, speed of passage, rainfall and runoff related to the characteristics of a cyclone to examine and verify the theoretical discussion presented in previous literatures with respect to the impact of a VSCS on the water quality of estuaries and lagoons.

The results revealed that *Phailin* had a much severe effect on the overall turbidity gradient of Chilika Lagoon compared with *Hudhud*. The analysis of MODIS images indicated that the saturated land pre-*Phailin* due to continuous heavy rainfall led to very high surface runoff after the landfall compared with post-*Hudhud*. Angles et al. (2015) suggested that the environmental condition pre-and post-cyclone will primarily determine its impact on estuaries and lagoons. Also, close proximity of *Phailin*'s landfall to Chilika Lagoon (~45 km), and its track towards the watershed of the lagoon triggered the higher surface runoff which probably led to higher turbidity compared with *Hudhud* that made landfall farther (~338 km) and

moved away from the lagoon as it progressed after the landfall. Srichandan et al. (2015b) also reported very high turbidity levels in Chilika Lagoon post-*Phailin* (221.4 NTU) compared with pre-*Phailin* (32.8 NTU). The northern catchment which includes agricultural land, bare ground and urban areas, primarily contributed to the surface runoff compared with the western watershed, which is mainly comprised forested land. Also, the downward sloping topography and major tributaries of Mahanadi River of NC support higher surface runoff and the Khallikote forest present in the WC of the lagoon limits the surface runoff to a large extent (Kumar et al. 2016). All of the above meteorological factors (rainfall intensity, rainfall amount, rainfall duration, distribution of rainfall over the drainage basin, direction of storm movement, earlier precipitation and soil moisture) and physical characteristics (land use, land cover, vegetation, topography) are listed by US Geological Survey (USGS) as governing parameters for controlling surface runoff (http://water.usgs.gov/edu/watercyclerunoff.html). Previous studies also documented relatively higher runoff in agricultural and urbanised watershed which elevated nutrients and suspended sediments to nearby water bodies (Jordan et al. 2003; Mallin and Corbett 2006; Mallin et al. 2009; Wetz and Yoskowitz 2013). One important difference observed between the two cyclones was the speed of passage which is characterised as a determining factor associated with the magnitude of impact of such VSCSs in previous literatures (Mallin and Corbett 2006; Srichandan et al. 2015b). For example, Mallin and Corbett (2006) observed that the fast moving hurricane *Andrew* resulted in low erosion compared with hurricane *Dennis* which lingered for several days over the watershed near North Carolina and resulted in enhanced runoff. The speed of passage for *Hudhud* was much faster (∼9–12 h) compared with *Phailin* (>24 h) over the watershed of Chilika, which caused the difference in rainfall amount and duration. This difference led to the highly variable surface runoff from the watershed of the lagoon and consequently, the magnitude of sediment transport to the lagoon was observed to be significantly different in both cases. *Phailin* made the entire lagoon highly turbid eliminating the usual clear-cut sector-wise turbidity gradient typical to Chilika; however, no such magnitude increment in turbidity was observed post-*Hudhud*.

The difference in precipitation and surface runoff in the catchments further led to sector-wise differential impact in TSS and Chl-*a* that are considered the primary indicators of water quality of any lagoon. The rainfall rate and surface runoff to the lagoon was much higher during the *Phailin* compared with *Hudhud*. The NS and CS were the most affected sectors with high TSS concentration post-*Phailin* due to significantly high surface runoff in combination with regular riverine input from seven major rivers (Kusumi, Tarimi, Mangalajodi, Makara, Daya, Nuna and Bhargavi) contributing large amount of sediment load to the lagoon from the northern side (Ghosh

et al. 2006). However, SS was the least affected region in terms of TSS probably due to the low surface runoff from WC due to the presence of forest and only one connecting river (Langeleswar) (Kumar et al. 2016). Massive increase in turbidity in the water column after *Phailin* reduced the transparency level and limited the availability of light (Srichandan et al. 2015b). The magnitude and spatial distribution of turbidity in the lagoon on the aftermath of these cyclones are primarily determined by wind speed and runoff. While massive runoff resulting from heavy rainfall brings substantial amount of sediments to the lagoon and can be considered the primary driver of turbidity, high wind speed triggers sediment re-suspension and is a secondary source of turbidity. Kumar et al. (2016) observed that above a threshold value of 6.5 m/s (23.4 km/h) wind intensity, re-suspension of sediments occurs in Chilika. In another study, Chen et al. (2007) also documented re-suspension of bottom sediments in Tampa Bay, Florida above a wind speed threshold limit of 6 m/s (21.6 km/h). Wind speed which plays the major role in sediment re-suspension during such cyclonic events (Chen et al. 2009; Wetz and Yoskowitz 2013) was significantly higher during *Phailin* compared with *Hudhud* which may have triggered additional turbidity in the lagoon. It is important to break down and analyse the physical and meteorological factors because they are strongly linked to the turbidity which is ultimately linked to the likelihood of an algal bloom after the passage of a cyclone. Wind induced bottom sediment re-suspension is also dependent on sediment types and size (Havens et al. 2011). The sediment size varies in different sectors of Chilika Lagoon such as fine sediments (silt and clay) in offshore (NS and CS) due to major river extracts and coarser sediment (sand) in nearshore (SS and OC) because of exchange of sea water through the mouth (Raman et al. 2007; Ansari et al. 2015). Therefore, NS and CS which are dominated by fine sediment experienced higher degree of re-suspension leading to high turbidity compared with SS. Havens et al. (2011) reported similar phenomena that fine sediments in central part of Lake Okeechobee were more susceptible to re-suspension after increases in wind velocity and caused more limitation of light compared with near-shore coarse sediment.

The limited light availability affected the Chl-*a* concentration, an indicator of primary productivity, which reduced significantly post-*Phailin* in all the sectors of the lagoon. Srichandan et al. (2015b) also reported a significant decrease in Chl-*a* concentration immediately after *Phailin* in Chilika Lagoon and no sign of phytoplankton bloom after the passage. Previous studies also reported reduced phytoplankton biomass after the passage of cyclone due to significant light attenuation in water column (Paerl et al. 1998; Mallin et al. 2002; Mallin and Corbett 2006; Srichandan et al. 2015b). On the other hand, this result was in contradiction to many previous literatures that reported enhanced phytoplankton biomass after the passage of cyclones or a anthropogenic massive runoff

(Angles et al. 2015; Sarangi et al. 2014; Huang et al. 2011; Mishra and Mishra 2010; Paerl et al. 2001, 2006; Mallin et al. 2006; Peierls et al. 2003). For example, similar increase was reported in recent studies by Sarangi et al. (2014) and Lotliker et al. (2014) in north-west region of BOB post-*Phailin*. Both studies correlated sea surface temperature (SST) with Chl-*a* concentration and concluded that enhanced nutrient supply due to mixing of water column and stratification of layer created a favourable condition for phytoplankton growth. However, Chilika is a shallow lagoon (depth range, 0.5–3.0 m) where stratification is not a major problem and there has been no evidence of stratification in the lagoon based on 12 years of data (2000–2011) analysed by CDA (Kumar and Pattnaik 2012). On the other hand, mixing of water column due to high wind action during cyclonic events may circulate large amount of nutrients from bottom of the lagoon to upper layers. These nutrients help proliferate phytoplankton growth if environmental conditions are supportive such as sufficient light, calm wind and low flushing rate. These favourable environmental conditions were not available post-*Phailin* which restricted the phytoplankton growth. Additionally, Bacillariophyta and Dinophyta are the dominant phytoplankton species in the lagoon which require highly saline and transparent waters to grow, but their growth rate, presented in the form of Chl-*a* following examples from Paerl et al. (2001), was restricted post-*Phailin* because of very high freshwater discharge and storm water runoff which reduced salinity and increased turbidity to a great extent in the lagoon (Srichandan et al. 2015b). Since Chl-*a* does not provide any indication about phytoplankton species composition, it is not possible to pinpoint the dominant species without field data. Other studies have also concluded that re-suspension of the sediments increases the nutrient availability which triggers algal growth (Zhu et al. 2014; Sarangi et al. 2014). However, that was not the case after *Phailin*. Turbidity in the lagoon started reducing as the days progressed after the passage of *Phailin* because the sediment started settling down to the bottom (Kumar et al. 2016) and consequently, Chl-*a* concentration recovered back to pre-cyclone level after a week of the passage, but a phytoplankton bloom was not observed.

In contrast, *Hudhud* made landfall relatively at farther distance from Chilika, stayed for shorter duration and moved away from the lagoon after its landfall. The combination of landfall location, duration and trajectory during *Hudhud* resulted in lower precipitation and surface runoff in the watershed of the lagoon. As a result, any sector of the lagoon did not experience an increase in TSS to the level of post-*Phailin*. However, through satellite imagery a phytoplankton bloom was observed with Chl-*a* concentration increasing three times after the passage of *Hudhud*. It could be related to the combined effect of light availability and nutrient enrichment in the water column, just suitable enough to favour the phytoplankton growth. For example, field data collected from the lagoon

suggested that there was about 10-fold increase in nitrate concentration in Chilika lagoon after *Hudhud* compared with pre-*Hudhud* month. The turbidity of the lagoon in September 2014 was 138 NTU which decreased to 95.4 NTU in October 2014 after *Hudhud*. The reduced turbidity (increased transparency) along with other favourable meteorological, physical and hydrological factors (calm wind, low precipitation, discharge, runoff and low flushing rate) created suitable environment for phytoplankton growth as evidenced with the fact that average phytoplankton density before *Hudhud* (September 2014) was 2200 cells/mL which increased to 6216 cells/mL after *Hudhud* (October 2014). Previous studies also suggested that when there is sufficient light available in the water column followed by tropical cyclone, stimulation of phytoplankton becomes more rapid (Miller et al. 2006; Wetz and Paerl 2008; Wetz and Yoskowitz 2013). Chilika Lagoon experienced a sudden increase in Chl-*a* just after 2 days of landfall of *Hudhud* and the upward trend continued for a few more days. This type of sudden increase in Chl-*a* is common in previous studies (Peierls et al. 2003; Paerl et al. 2010; Huang et al. 2011; Sarangi et al. 2014; Lotliker et al. 2014; Baliarsingh et al. 2015). For example, Huang et al. (2011) reported sudden increase in mean Chl-*a* from 5.3 to 14.7 µg/L in Pensacola Bay, Florida just after a day of passage of Hurricane *Ivan*. In another study, Baliarsingh et al. (2014) reported a significant increase in Chl-*a* just after 3 days of landfall of *Hudhud* in north-western BOB from 1.58–2.28 to 2.57–6.62 mg/m^3. They attributed this increase to nutrient entrainment from river influx and mixing due to the VSCS. Zhu et al. (2014) used hourly in situ data and found short-term (on the order of hours) nutrient pulsing as a major factor for bloom during the passage of a cyclone. Other studies conducted in situ experiments and observed variation in phytoplankton density within hours because of nutrient pulses (Collos 1986; Pinckney et al. 1999). This process of mixing of water column and nutrient pulsing are fairly short-term phenomena and to capture this, very high temporal resolution (probably hourly) data is required (Nishino et al. 2015; Marra et al. 2015). Thick cloud cover during the cyclones and 1-day revisit period of MODIS Terra satellite did not allow capturing such short-term variability in water quality. But a gradual spread in the spatial coverage of increased Chl-*a* concentration from SS towards NS was clearly visible in post-*Hudhud* MODIS-derived Chl-*a* maps (Fig. 9).

In the above discussion, a combination of several factors was attributed to the differential impact of two cyclones on the water quality of the lagoon. However, isolating a single factor primarily responsible for the differential impact would not be useful because each individual factor has its own importance and often correlated with other factors. For example, distance from landfall location cannot be isolated from the trajectory and speed of the cyclone. Past studies have reported that even if a cyclone makes landfall close to a study area but passes

very quickly, then it would not bring as much amount of rainfall and runoff compared with a slow-moving cyclone which stayed for a longer duration (Mallin and Corbett 2006). Similarly, surface runoff cannot be isolated from precipitation, nutrient pulsing cannot be isolated from mixing of water column. The same principle is applicable to the phytoplankton growth in a lagoon which requires a combination of several factors favourable for primary production. Srichandan et al. (2015b) suggested that several other factors such as nutrient, turbidity, water residence time and flushing rate are equally important for phytoplankton biomass production along with geographic-geomorphologic-bathymetric setting of an estuary. For instance, high flushing rate in combination with high fresh water discharge limited the phytoplankton growth in Neuse River Estuary post-Hurricane *Fran* (Paerl et al. 1998). Similarly, rapid flushing for several weeks was reported post-*Phailin* in Chilika Lagoon that slowed the rate of phytoplankton growth (Srichandan et al. 2015b). Flushing rate

was comparatively less rapid post-*Hudhud* as the flood intensities in the distributaries were much lower compared with *Phailin*. Another factor suggested by Wetz and Yoskowitz (2013) was calm wind after the passage of cyclone supports the stratification and light condition for phytoplankton growth. The wind speed was stable after the passage of *Hudhud* but wind speed was dynamic post-*Phailin* that might have slowed down the phytoplankton growth in the lagoon. Therefore, lower rainfall, lower surface runoff, less turbidity, low flushing rate and stable wind, all favoured the phytoplankton bloom post-*Hudhud*. The same factors but at a different magnitude prevented a phytoplankton bloom post-*Phailin*. The above results and discussions validated the proposed hypothesis that the likelihood of a phytoplankton bloom or significant increase in phytoplankton biomass after a cyclone is dependent on the physical, meteorological and geomorphological characteristics of the VSCS and the lagoon (Fig. 11).
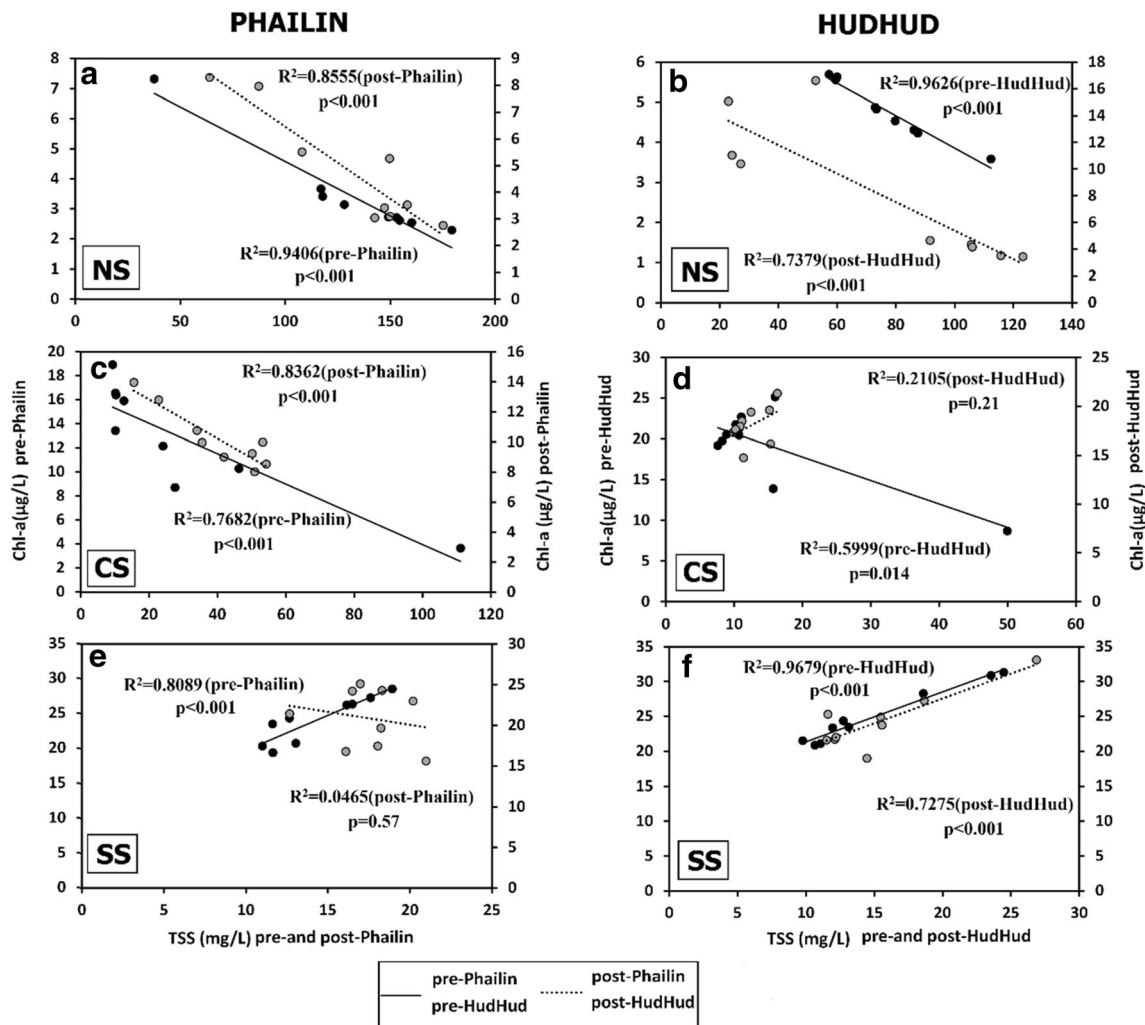

Fig. 11 Correlation between mean TSS and mean Chl-*a* concentration pre- and post-VSCSs for NS, CS and SS. All locations were time averaged to obtain the average TSS and Chl-*a*. The *solid trend lines* with *dark circles* correspond to pre-VSCS, and *dashed trend lines* with *light circles* represent post-VSCS data

Conclusion

This paper dealt with questions such as why some cyclones trigger phytoplankton blooms in estuaries and lagoons and some do not? and what factors control the likelihood of a bloom after the passage of a cyclonic storm? A comprehensive comparative analysis of several factors was performed to isolate the causes of the differential impact of anniversary VSCSs, *Phailin* and *Hudhud*, on the water quality of Chilika Lagoon. The anniversary VSCSs allowed the verification of a theoretical concept widely discussed in previous literatures that characteristics of a cyclone such as close landfall location, high wind intensity, longer duration of stay, trajectories along the watershed of study area would support high precipitation and surface runoff which may lead to increased turbidity and a phytoplankton bloom in nearby water bodies such as estuaries and lagoons (Wetz and Yoskowitz 2013; Mallin and Corbrett 2006; Paerl et al. 2001). *Phailin*'s impact on Chilika Lagoon and its watershed resulted in unprecedented levels of precipitation and runoff before-during-after the landfall, which shattered the typical sectorial turbidity gradient. Exponential increase in turbidity because of a combination of runoff and wind-driven re-suspension of fine sediments resulted in strong attenuation of light in water column post-*Phailin*. Limited light condition coupled with enhanced flushing rate due to flooded river and increased fresh water discharge reduced the Chl-*a* concentration after the passage of *Phailin*. In contrast, relatively farther landfall location, trajectory away from the lagoon, relatively lower wind intensity and short duration of stay of VSCS *Hudhud*, led to lesser precipitation and surface runoff compared with *Phailin*. Consequently, lagoon did not experience a drastic increase in turbidity and light attenuation. Sufficient light availability, stable wind, reduced flushing all favoured the phytoplankton growth after passage of *Hudhud* and as a result, Chl-*a* concentration increased almost 3-fold in all the sectors of the lagoon.

The frequency of tropical cyclones is expected to increase under the global climate change scenario which makes satellite-based high spatial and temporal assessment very useful compared with field sampling program, which are limited in spatial and temporal domain (Srichandan et al. 2015b). Satellite data coupled with model-derived products may become very useful in near future for the assessment of cyclone induced impact and predicting phytoplankton bloom prone areas. The approach used in this study can be applied to other cyclone-prone coastal areas. Coupling of satellite based observation with modelling output from systems such as Giovanni can improve monitoring program implemented in numerous coastal estuaries and lagoons. Susceptible watershed areas that contribute in high surface runoff can be isolated and management plan can be implemented like creating buffer zone or plantation to minimise the surface erosion rate, which is a major factor in deteriorating water quality of any lake. Also,

long-term monitoring ability of satellite-based model will facilitate researchers and regulators to assess the changes in estuarine and lake system and associated watershed on a broader scale. The ability to predict these changes on estuarine and coastal environments might become an essential part of designing and implementing the management and restoration effort for a lake, estuary, or coastal region in future. The recent advancement in sensors and technologies will provide researchers valuable data at a high temporal granularity to evaluate the impact of cyclones on water quality of lakes and estuaries even more precisely (Glasgow et al. 2004). Similarly, satellite data coupled with land surface models such as Giovanni based hourly products can help to a great extent to monitor changes in watershed characteristics and worldwide climate patterns during cyclonic events in near future.

References

Acker, J., and G. Leptoukh. 2007. Online analysis enhances use of NASA earth science data. *Eos Transaction. American Geophysical Union* 88(2): 14–17.

Acker, J., R. Soebiyanto, R. Kiang, and S. Kempler. 2014. Use of the NASA Giovanni data system for geospatial public health research: example of weather-influenza connection. *ISPRS International Journal of Geo-Information* 3: 1372–1386.

Angles, S., A. Jordi, and L. Campbell. 2015. Responses of the coastal phytoplankton community to tropical cyclones revealed by high-frequency imaging flow cytometry. *Limnology and Oceanography* 60: 1562–1576.

Ansari, K.G.M.T., A.K. Pattnaik, G. Rastogi, and P. Bhadury. 2015. An inventory of free-living marine nematodes from Asia's largest coastal lagoon, Chilika, India. *Wetlands Ecology and Management* 23(2). doi:10.1007/s11273-015-9426-2.

Babin, S.M., J.A. Carton, T.D. Dickey, and J.D. Wiggert. 2004. Satellite evidence of hurricane induced phytoplankton blooms in an oceanic desert. *Journal of Geophysical Research* 109. doi:10.1029/2003JC001938.

Baliarsingh, S.K., C. Parida, A.A. Lotliker, S. Srichandan, K.C. Sahu, and T.S. Kumar. 2015. Biological implications of cyclone Hudhud in the coastal waters of northwestern Bay of Bengal. *Current Science* 109(7): 1243–1245.

Binding, C.E., D.G. Bowers, and E.G. Mitchelson-Jacob. 2005. Estimating suspended sediment concentration from ocean colour measurements in moderately turbid waters; the impact of variable particle scattering properties. *Remote Sensing of Environment* 94: 373–383.

Chen, Z., C. Hu, and F. Muller-Karger. 2007. Monitoring turbidity in Tampa Bay using MODIS/Aqua 250-m imagery. *Remote Sensing of Environment* 109: 207–220.

Chen, S., W. Huang, H. Wang, and D. Li. 2009. Remote sensing assessment of sediment re-suspension during Hurricane Frances in

Apalachicola Bay, USA. *Remote Sensing of Environment* 113: 2670–2681.

Chen, S.S., W.R. Huang, W.Q. Chen, and X.Z. Chen. 2011. An enhanced MODIS remote sensing model for detecting rainfall effects on sediment plume in the coastal waters of Apalachicola Bay. *Marine Environmental Research* 72(5): 265–272.

Collos, Y. 1986. Time-lag algal growth dynamics: biological constraints on primary production in aquatic environments. *Marine Ecology-Progress Series* 33: 193–206.

Cui, L., Y. Qiu, T. Fei, Y. Liu, and G. Wu. 2013. Using remotely sensed suspended sediment concentration variation to improve management of Poyang Lake, China. *Lake and Reservoir Management* 29: 47–60.

Dickey, T.D., G.C. Chang, Y.C. Agrawal, A.J. Williams, and P.S. Hill. 1998. Sediment resuspension in the wakes of hurricanes Edouard and Hortense. *Geophysical Research Letter* 25: 3533–3536.

Dogliotti, A.I., K.G. Ruddick, B. Nechad, D. Doxaran, and E. Knaeps. 2015. A single algorithm to retrieve turbidity from remotely-sensed data in all coastal and estuarine waters. *Remote sensing of. Environment* 156: 157–168.

El-Alem, A., K. Chokmani, I. Laurion, and S.E. El-Adlouni. 2012. Comparative analysis of four models to estimate chlorophyll-a concentration in case-2 waters using MODerate resolution imaging Spectroradiometer (MODIS) imagery. *Remote Sensing* 4: 2373–2400.

Fang, H., P. L. Hrubiak, H. Kato, M. Rodell, W. L. Teng and B. E. Vollmer. 2008. Global Land Data Assimilation System (GLDAS) products from NASA Hydrology Data and Information Services Center (HDISC). ASPRS 2008 Annual Conference Portland, Oregon 28 April–2 May 2008. http://www.asprs.org/a/publications/proceedings/portland08/0020.pdf

Fogel, M., C. Aguilar, R. Cuhel, D. Hollander, J. Willey, and H. Paerl. 1999. Biological and isotopic changes in coastal waters induced by hurricane Gordon. *Limnology and Oceanography* 44(6): 1359–1369.

Fox, R.C., and K.M. Rowntree. 2013. Extreme weather events in the Sneeuberg, Karoo, South Africa: a case study of the floods of 9 and 12 February 2011. *Hydrology and Earth System Sciences Discussion* 10: 10809–10844.

Ghosh, A.K., A.K. Pattnaik, and T.J. Ballatore. 2006. Chilika lagoon: restoring ecological balance and livelihoods through re-salinization. *Lakes & Reservoirs: Research and Management* 11: 239–255.

Gitelson, A.A., Y. Gritz, and M.N. Merzlyak. 2003. Relationships between leaf chlorophyll content and spectral reflectance and algorithms for non-destructive chlorophyll assessment in higher plant leaves. *Journal of Plant Physiology* 160: 271–282.

Glasgow, H.B., J.M. Burkholder, R.E. Reed, A.J. Lewitus, and J.E. Kleinman. 2004. Real-time monitoring of water quality: a review of current applications, and advancements in sensor, telemetry, and computing techniques. *Journal of Experimental Marine Biology and Ecology* 300: 409–448.

GoO, 2013. Memorandum on the Very Severe Cyclone Phailin and the Subsequent Flood 12–15 October 2013. The Revenue and Disaster Management Department Government of Odisha. http://www.osdma.org/userfiles/file/MEMORANDUMPhailin.pdf . Accessed 10 October 2014.

Gupta, M. 2013. Chromaticity analysis of the Chilika lagoon for total suspended sediment estimation using RESOURCESAT-1 AWiFS data—a case study. *Journal of Great Lakes Research* 39: 696–700.

Gupta, G.V.M., V.V.S.S. Sarma, R.S. Robin, A.V. Raman, M.J. Kumar, M. Rakesh, and B.R. Subramanian. 2008. Influence of net ecosystem metabolism in transferring riverine organic carbon to atmospheric CO_2 in a tropical coastal lagoon (Chilka Lake, India. *Biogeochemistry* 87(3): 265–285.

Havens, K.E., J.R. Beaver, D.A. Casamatta, T.L. East, R.T. James, P. Mccormick, E.J. Phlips, and A.J. Rodusky. 2011. Hurricane effects on the planktonic food web of a large subtropical lake. *Journal of Plankton Research* 33: 1081–1094.

Hu, C.M. 2009. A novel ocean color index to detect floating algae in the global oceans. *Remote Sensing of Environment* 113(10): 2118–2129.

Hu, C., Z. Chen, T. Clayton, P. Swarnzenski, J. Brock, and F. Muller-Karger. 2004. Assessment of estuarine water quality indicators using MODIS medium-resolution bands: initial results from Tampa Bay, Florida. *Remote Sensing of Environment* 93: 423–441.

Huang, W., D. Mukherjee, and S. Chen. 2011. Assessment of Hurricane Ivan impact on chlorophyll-a in Pensacola Bay by MODIS 250 m remote sensing. *Marine Pollution Bulletin* 62(3): 490–498.

IFRC, 1999. Cyclone: Orissa, India Information Bulletin No. 1. *International Federation of Red Cross (IFRC) and Red Crescent Societies*. http://www.ifrc.org/docs/appeals/rpts99/in005.pdf. Accessed 10 October 2014.

IMD, 2013. Very severe cyclonic storm, PHAILIN over the Bay of Bengal (08–14 October 2013): a report. http://www.imd.gov.in/section/nhac/dynamic/phailin.pdf.

IMD, 2014. Very severe cyclonic storm, HUDHUD over the Bay of Bengal (07–14 October 2014): A Report. http://www.rsmcnewdelhi.imd.gov.in/images/pdf/publications/preliminary-report/hud.pdf.

Jordan, T.E., D.F. Whigham, K.H. Hofmockel, and M.A. Pittek. 2003. Wetlands and aquatic processes: nutrient and sediment removal by a restored wetland receiving agricultural runoff. *Journal of Environmental Quality* 32: 1534–1547.

Kahru, M., B.G. Mitchell, A. Diaz, and M. Miura. 2004. Modis detects a devastating algal bloom in Paracas Bay, Peru. *Eos* 85(45): 465–472.

Kumar, R. and A.K. Pattnaik. 2012. Chilika—an integrated management planning framework for conservation and wise use. Wetlands International-South Asia, New Delhi, India and Chilika Development Authority, Bhubaneswar, India.

Kumar, A., S. Equeenuddin, D.R. Mishra, and B.C. Acharya. 2016. Remote monitoring of sediment dynamics in a coastal lagoon: long-term spatio-temporal variability of suspended sediment in Chilika. *Estuarine Coastal and Shelf. Science* 170: 155–172.

Lahet, F., and D. Stramski. 2010. MODIS imagery of turbid plumes in San Diego coastal waters during rainstorm events. *Remote Sensing of Environment* 114: 332–344.

Leptoukh, G., S. Berrick, H. Rui, Z. Liu, T. Zhu and S. Shen. 2005. NASA GES DISC On-line visualization and analysis system for gridded remote sensing data. In: Proceedings of the 31th International Symposium of Remote Sensing of the Environment (ISRSE), St. Petersburg, Russia.

Lin, I., W.T. Liu, C.C. Wu, G.T.F. Wong, C. Hu, Z. Chen, W.D. Liang, Y. Yang, and K.K. Liu. 2003. New evidence for enhanced ocean primary production triggered by tropical cyclone. *Geophysical Research Letter* 30(13): 1718. doi:10.1029/2003GL017141.

Liu, C.D., B.Y. He, M.T. Li, and X.Y. Ren. 2006. Quantitative modeling of suspended sediment in middle Changjiang River from MODIS. *Chinese Geographical Science* 16(1): 79–82.

Loherenz, S.E., W. Cai, X. Chen, and M. Tuel. 2008. Satellite assessment of bio-optical properties of Northern Gulf of Mexico coastal waters following Hurricanes Katrina and Rita. *Sensors* 8: 4135–4150.

Lotliker, A.A., T. Srinivasakumar, V.S. Reddem, and S. Nayak. 2014. Cyclone Phailin enhanced the productivity following its passage: evidence from satellite data. *Current Science.* 106(3): 360–361.

Mallin, M.A., M.H. Posey, M.R. McIver, D.C. Parsons, S.H. Ensign, and T.D. Alphin. 2002. Impacts and recovery from multiple hurricanes in a Piedmont-coastal plain river system. *Bioscience* 52: 999–1010.

Mallin, M.A., and C.A. Corbrett. 2006. How hurricane attributes determine the extent of environmental effects: multiple hurricanes and different coastal systems. *Estuaries and Coasts* 29: 1046–1061.

Mallin, M.A., V.L. Johnson, S.H. Ensign, and T.A. MacPherson. 2006. Factors contributing to hypoxia in rivers, lakes and streams. *Limnology and Oceanography* 51(2): 690–701.

Marra, J.F., T.D. Dickey, A.J. Plueddemann, R.A. Weller, C.S. Kinkade, and M. Stramska. 2015. Phytoplankton bloom phenomena in the North Atlantic Ocean and Arabian Sea ICES. *Journal of Marine Science*. doi:10.1093/icesjms/fsu241.

Matarrese, R., E. Vermote and M. Kearney. 2005. Impact of Hurricane Isabel on the water properties of the Chesapeake Bay Area. Hurricane Isabel in perspective. Chesapeake Research Consortium, CRC Publication 05–160, Edgewater, MD.

Miller, R.L., and B.A. McKee. 2004. Using MODIS 250 m imagery to map concentration of total suspended matter in coastal waters. *Remote Sensing of Environment* 93: 259–266.

Miller, R.L., C.C. Liu, C.J. Buonassissi, and A.M. Wu. 2011. A multi-sensor approach to examining the distribution of Total suspended matter (TSM) in the Albemarle-Pamlico estuarine system, NC, USA. *Remote Sensing* 3: 962–974.

Miller, W.D., L.W. Harding, and J.E. Adolf. 2006. Hurricane Isabel generated an unusual fall bloom in Chesapeake Bay. *Geophysical Research Letter* 33: L06612. doi:10.1029/2005GL025658.

Mishra, S., and D.R. Mishra. 2012. Normalized difference chlorophyll index: a novel model 1110 for remote estimation of chlorophyll-a concentration in turbid productive waters. *Remote Sensing of Environment* 117: 394–406.

Mishra, D.R., and S. Mishra. 2010. Plume and bloom: effect of the Mississippi River diversion on the water quality of Lake Pontchartrain. *Geocarto International*. doi:10.1080/10106041003763394.

Mishra, S.P., and D.R. Panigrahi. 2014. Storm impact on South Odisha coast, India. *International Journal of Advance Research in Science and Engineering* 3(11) ISSN: 2319-8354 (E).

Nayak, S.R., R.K. Sarangi, and A.S. Rajwat. 2001. Application of IRS-P4 OCM data to study the impact of cyclone on coastal environment of Orissa. *Current Science* 80: 1208–1212.

Nishino, S., Y. Kawaguchi, J. Inoue, T. Hirawake, A. Fujiwara, R. Futsuki, J. Onodera, and M. Aoyama. 2015. Nutrient supply and biological response to wind-induced mixing, inertial motion, internal waves, and currents in the northern Chukchi Sea. *Journal of Geophysical Research.* 120: 1975–1992.

Ondrusek, M., E. Stengel, C.S. Kinkade, R.L. Vogel, P. Keegstra, C. Hunter, and C. Kim. 2012. The development of a new optical total suspended matter algorithm for the Chesapeake Bay. *Remote Sensing of Environment* 119: 243–254.

Paerl, H.W., J.L. Pinckney, J.M. Fear, and B.L. Peierls. 1998. Ecosystem responses to internal and watershed organic matter loading: consequences for hypoxia in the eutrophying Neuse River estuary, North Carolina, USA. *Marine Ecology Progress Series* 166: 17–25.

Paerl, H.W., J.D. Bales, L.W. Ausley, C.P. Buzzelli, L.B. Crowder, L.A. Eby, J.M. Fear, M. Go, B.L. Peierls, T.L. Richardson, and J.S. Ramus. 2001. Ecosystem impacts of 3 sequential hurricanes (Dennis, Floyd and Irene) on the US's largest lagoonal estuary, Pamlico sound. *NC. Proceedings of the National Academy of Science. USA.* 98(10): 5655–5660.

Paerl, H.W., L.M. Valdes, B.L. Peierls, J.E. Adolf, and L.W. Harding. 2006. Anthropogenic and climatic influences on the eutrophication of large estuarine ecosystems. *Limnology and Oceanography* 51: 448–462.

Paerl, H.W., K.L. Rossignol, S.N. Hall, B.L. Peierls, and M.S. Wetz. 2010. Phytoplankton community indicators of short- and long term ecological change in the anthropogenically and climatically impacted Neuse River estuary, NorthCarolina, USA. *Estuaries and Coasts* 33: 485–497.

Peierls, B., R. Christian, and H. Paerl. 2003. Water quality and phytoplankton as indicators of hurricane impacts on a large estuarine ecosystem. *Estuaries* 26: 1329–1343.

Petus, C., G. Chust, F. Gohin, D. Doxaran, J.M. Froidefond, and Y. Sagarminaga. 2010. Estimating turbidity and total suspended matter in the Adour River Plume (South Bay of Biscay) using MODIS 250-m imagery. *Continental Shelf Research* 30: 379–392.

Pinckney, J.L., H.W. Paerl, and M.B. Harrington. 1999. Responses of the phytoplankton community growth rate to nutrient pulses in variable estuarine environments. *Journal of Phycology* 35: 1455–1463.

Raman, A.V., C. Kalavati and Y. Prabhakara Rao. 2007. Modelling Chilka Lake: an ecosystem approach. Final report (2004–07) Submitted to Ministry of Earth Sciences ICMAM Directorate Chennai. http://www.icmam.gov.in/CHIL.PDF.

Rodell, M., and P.R. Houser. 2004. Updating a land surface model with MODIS derived snow cover. *Journal of Hydrometeorology* 5(6): 1064–1075.

Shi, W., and M. Wang. 2008. Three-dimensional observations from MODIS and CALIPSO for ocean responses to cyclone Nargis in the Gulf of Martaban. *Geophysical Research Letter* 35: L21603. doi:10.1029/2008GL035279.

Sarangi, R.K., M.K. Mishra, and P. Chauhan. 2014. Remote sensing observations on impact of Phailin cyclone on phytoplankton distribution in northern Bay of Bengal. *IEEE Journal of Selected Topic in Applied Earth Observation and Remote Sensing* 8(2): 539–549.

Sahoo, S., S.K. Baliarsingh, A.A. Lotiker, and K.C. Sahu. 2014. Imprint of cyclone Phailin on water quality of Chilika lagoon. *Current Science* 107(9): 1380–1381.

Srichandan, S., J.Y. Kim, P. Bhadury, S.K. Barik, P.R. Muduli, R.N. Samal, A.K. Pattnaik, and G. Rastogi. 2015a. Spatiotemporal distribution and composition of phytoplankton assemblages in a coastal tropical lagoon: Chilika, India. *Environmental Monitoring and Assessment* 187(47): 1–17.

Srichandan, S., J.Y. Kim, A. Kumar, D.R. Mishra, P. Bhadury, P.R. Muduli, A.K. Pattnaik, and G. Rastogi. 2015b. Interannual and cyclone-driven variability in phytoplankton communities of a tropical coastal lagoon. *Marine Pollution Bulletin* 101(1): 39–52.

Tarrant, P.E., J.A. Amacher, and S. Neuer. 2010. Assessing the potential of medium-resolution imaging spectrometer (MERIS) and moderate-resolution imaging Spectroradiometer (MODIS) data for monitoring total suspended matter in small and intermediate sized lakes and reservoirs. *Water Resources Research* 46(9).

UNEP, 2013. Cyclone Phailin in India: early warning and timely actions saved lives. http://www.unep.org/pdf/UNEP_GEAS_NOV_2013.pdf.

Wang, M., C.J. Nim, S.H. Son, and W. Shi. 2012. Characterization of turbidity in Florida's Lake Okeechobee and Caloosahatchee and St. Lucie estuaries using MODIS-aqua measurements. *Water Research* 46: 5410–5422.

Wetz, M.S., and H.W. Paerl. 2008. Estuarine phytoplankton responses to hurricanes and tropical storms with different characteristics (trajectory, rainfall, winds. *Estuaries and Coasts* 31: 419–429.

Wetz, M.S., and D.W. Yoskowitz. 2013. An 'extreme' future for estuaries? Effects of extreme climatic events on estuarine water quality and ecology. *Marine Pollution Bulletin* 69(2013): 7–18.

Wu, G., L. Cui, J. He, H. Duan, T. Fei, and Y. Liu. 2013. Comparison of MODIS-based models for retrieving suspended particulate matter concentration in Poyang Lake, China. *International Journal of Applied Earth Observation and Geoinformation* 24: 63–72.

Zhang, Y., S. Lin, J. Liu, X. Qian, and Y. Ge. 2010. Time-series MODIS image-based retrieval and distribution analysis of total suspended matter concentrations in Lake Taihu (China. *International Journal of Environmental Research and Public Health.* 7(9): 3545–3560.

Zhang, Y., S. Lin, X. Qian, Q. Wang, Y. Qian, J. Liu, and Y. Ge. 2011. Temporal and spatial variability of chlorophyll a concentration in Lake Taihu using MODIS time-series data. *Hydrobiologia* 661: 235–250.

Zhao, H.H., Q. Chen, N.D. Walker, Q.A. Zheng, and H.L. MacIntyre. 2011. A study of sediment transport in a shallow estuary using MODIS imagery and particle tracking simulation. *International Journal of Remote Sensing* 32(21): 6653–6671.

Zhu, M., H.W. Paerl, G. Zhu, T. Wu, W. Li, K. Shi, L. Zhao, Y. Zhang, B. Qin, and A.M. Caruso. 2014. The role of tropical cyclones in stimulating cyanobacterial blooms in hypertrophic Lake Taihu, China. *Harmful Algae* 39: 310–321.